

2

PL-TR-91-2004

AD-A236 030



The Transition to the Elastic Regime
in the Vicinity of an Underground Explosion

J. B. Minster
S. M. Day
P. M. Shearer

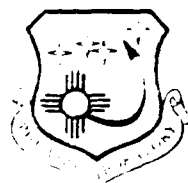
University of California, San Diego
Scripps Institute of Oceanography
IGPP, 9500 Gilman Drive
La Jolla, CA 92093-0225

18 November 1990

Scientific Report No. 2

APPROVED FOR PUBLIC RELEASE; DISTRIBUTION UNLIMITED

DTIC
ELECTE
MAY 13 1991
S E D



PHILLIPS LABORATORY
AIR FORCE SYSTEMS COMMAND
HANSCOM AIR FORCE BASE, MASSACHUSETTS 01731-5000



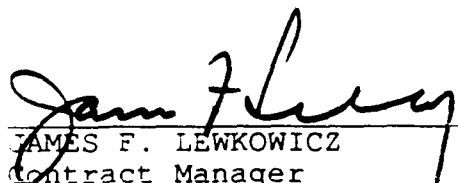
91 5 13 054

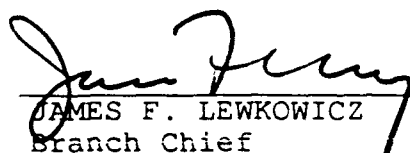
SPONSORED BY
Defense Advanced Research Projects Agency
Nuclear Monitoring Research Office
ARPA ORDER NO. 2309

MONITORED BY
Phillips Laboratory
F19628-88-K-0039

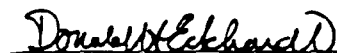
The views and conclusions contained in this document are those of the authors and should not be interpreted as representing the official policies, either expressed or implied, of the Defense Advanced Research Projects Agency or the U.S. Government.

This technical report has been reviewed and is approved for publication.


JAMES F. LEWKOWICZ
Contract Manager
Solid Earth Geophysics Branch
Earth Sciences Division


JAMES F. LEWKOWICZ
Branch Chief
Solid Earth Geophysics Branch
Earth Sciences Division

FOR THE COMMANDER


DONALD H. ECKHARDT, Director
Earth Sciences Division

This report has been reviewed by the ESD Public Affairs Office (PA) and is releasable to the National Technical Information Service (NTIS).

Qualified requestors may obtain additional copies from the Defense Technical Information Center. All others should apply to the National Technical Information Service.

If your address has changed, or if you wish to be removed from the mailing list, or if the addressee is no longer employed by your organization, please notify PL/IMA, Hanscom AFB, MA 01731-5000. This will assist us in maintaining a current mailing list.

Do not return copies of this report unless contractual obligations or notices on a specific document requires that it be returned.

REPORT DOCUMENTATION PAGE			Form Approved OMB No. 0704-0188	
<small>Public reporting burden for this collection of information is estimated to average 1 hour per response, including the time for reviewing instructions, searching existing data sources, gathering and maintaining the data needed, and completing and reviewing the collection of information. Send comments regarding this burden estimate or any other aspect of this collection of information, including suggestions for reducing this burden, to Washington Headquarters Services, Directorate for Information Operations and Reports, 1215 Jefferson Davis Highway, Suite 1204, Arlington, VA 22202-4302, and to the Office of Management and Budget, Paperwork Reduction Project (0704-0188), Washington, DC 20503.</small>				
1. AGENCY USE ONLY (Leave blank)		2. REPORT DATE 11/18/90		3. REPORT TYPE AND DATES COVERED Scientific # 2
4. TITLE AND SUBTITLE The Transition to the Elastic Regime in the Vicinity of an Underground Explosion			5. FUNDING NUMBERS PE 62714 E PR 8A10 TA DA WVAR Contract # F19628-88-K-0039	
6. AUTHOR(S) J.B. Minster, S.M. Day*, and P.M. Shearer				
7. PERFORMING ORGANIZATION NAME(S) AND ADDRESS(ES) Regents of the University of California University of California, San Diego Scripps Institution of Oceanography (0225) IGPP, 9500 Gilman Drive La Jolla, CA 92093-0225			8. PERFORMING ORGANIZATION REPORT NUMBER	
9. SPONSORING / MONITORING AGENCY NAME(S) AND ADDRESS(ES) Phillips Laboratory Hanscom AFB, MA 01731-5000 Contract Manager: James F. Lewkowicz/LWH			10. SPONSORING / MONITORING AGENCY REPORT NUMBER PL-TR-91-2004	
11. SUPPLEMENTARY NOTES *San Diego State University, Department of Geological Sciences, San Diego, CA 92182				
12a. DISTRIBUTION AVAILABILITY STATEMENT Approved for public release; distribution unlimited			12b. DISTRIBUTION CODE	
13. ABSTRACT (Maximum 200 words) <p>We have examined wave propagation problems in nonlinear materials for which attenuation, described by the inverse quality factor Q^{-1}, is independent of frequency but grows linearly with strain amplitude. This particular relationship is an adequate representation of many laboratory observations for rocks tested in the strain range 10^{-6} to 10^{-4}. However, our concern is that use of data reduction techniques developed in the context of a linear theory (e.g. spectral ratios, Lorentz peaks) may yield biased answers at these moderately high strains.</p> <p>The results of our elementary, one-dimensional numerical modeling experiments are mixed, and do not seem to be easily predictable from simple arguments. For example, Q^{-1} estimates derived from the half-width of a resonance peak appear to be surprisingly accurate well into the nonlinear regime. Similarly, the nonlinear interaction of one-dimensional pulses does not lead to strong departures from linear superposition in the range of nonlinear behavior we have considered. On the other hand, the propagation of a one-dimensional narrow pulse through a medium with frequency-independent, but amplitude-dependent Q is not described accurately by an equivalent "Q-operator", and observed resonance peak distortions due to nonlinearity are worse than predicted by the calculations. (over)</p>				
14. SUBJECT TERMS Rock mechanics, JVE, Source medium properties, Nonlinear attenuation			15. NUMBER OF PAGES 50	
			16. PRICE CODE	
17. SECURITY CLASSIFICATION OF REPORT unclassified	18. SECURITY CLASSIFICATION OF THIS PAGE unclassified	19. SECURITY CLASSIFICATION OF ABSTRACT unclassified	20. LIMITATION OF ABSTRACT SAR	

We rely on fully nonlinear finite difference simulations in which attenuation is independent of frequency but is proportional to the local strain amplitude. We find that, in contrast to linear Q models for which the spectrum of the " Q operator" tends to unity at low frequencies, a nonlinear rheology may lead to significant spectral distortions at all frequencies, and energy losses can be substantial even at wavelengths long compared to the propagation distance. Thus, even though this nonlinear rheology is only relevant in a limited range of scaled distances from a contained explosion, this raises the possibility that the far field source spectrum can be affected to some degree at all frequencies, including those pertinent to teleseismic body waves. In that case, nonlinear amplitude dependent attenuation would have to be taken into account when evaluating the effectiveness of seismic coupling. However, we show that extrapolation of our one-dimensional results to the spherically symmetric case is not straightforward. Nonlinear wave propagation is pulse-shape sensitive, and each individual problem must be tested separately in numerical simulations.

Accession For	
NTIS GRA&I	<input checked="" type="checkbox"/>
DTIC TAB	<input checked="" type="checkbox"/>
Unannounced	<input type="checkbox"/>
Justification	
By	
Distribution/	
Availability Codes	
Dist	Avail and/or Special
A-1	

Introduction

It is well documented from laboratory experiments that the attenuation of elastic waves is amplitude dependent at strains greater than 10^{-6} . There exists therefore an intermediate strain regime in which the deformation is not strong enough to cause macroscopic material failure, but is large enough to affect wave propagation. Because the rheology depends on amplitude, wave propagation is nonlinear, and reflects the influence of *inelastic* mechanisms. In the high-strain regime, these mechanisms dominate and control the rate of energy dissipation, but in the low-strain regime, their effects are masked by linear, amplitude independent *anelastic* mechanisms.

The nonlinearity means that the analytical tools usually employed to solve wave propagation problems are not valid in this intermediate-strain regime. This raises a number of questions regarding the acquisition and interpretation of experimental data. For instance:

- In resonating bar experiments, Lorentz peaks become quite distorted and asymmetric, and the interpretation of the half-power peak width in terms of Q^{-1} is not strictly valid, since the predicted width of the Lorentz peak stems from a linear perturbation treatment of the complex Helmholtz equation.
- In pulse propagation experiments, the use of spectral ratios to estimate Q^{-1} depends implicitly on the validity of a linear theory. The use of rise times as Q^{-1} estimators is also open to question since the relationship between rise time and attenuation has been derived only in the linear case.

Nevertheless, linear analysis of laboratory data which clearly exhibit nonlinear traits is attractive, in the sense that it yields fairly simple and apparently self-consistent results. Furthermore, a reasonable physical interpretation appears feasible: their own experiments have led *Stewart et al.* [1983] to propose a physical model based on Hertzian contacts across cracks which generalizes the earlier models of *Walsh* [1966] and *Mavko* [1979].

The nonlinear regime must prevail within a range of scaled distances from a contained explosive source, since strain amplitudes in the very near field are sufficient to cause material failure, while far-field radiation falls clearly in the linear low-amplitude regime. This intermediate strain, nonlinear zone contains the transition from what has traditionally been called the "elastic" radius in numerical source models to the far-field, low-strain (an)elastic regime. *Minster and Day* [1986] attempted to examine this and other issues by comparing the decay of peak displacements and velocities for the Cowboy series with laboratory results on salt obtained by *Tittman* [1983]. However, the algorithm they used is inadequate since it does not satisfy local conditions both in time and space, and thus is

nonphysical. A better algorithm can be devised using the Padé approximations developed by *Day and Minster* [1984, 1990], or the least-squares approximations of *Witte* [1989] and *Witte and Richards*, [1990], although any procedure which depends on selecting Q as a particular measure of (amplitude-dependent) attenuation is likely to be an inadequate representation of the true physical processes.

In this paper, we present a series of simple, one-dimensional numerical experiments designed to test the consistency of the models and laboratory results. When it comes to wave propagation in a nonlinear medium, intuition developed from linear Q models is a rather poor, often misleading guide, and our results are mixed, and do not seem to be easily predictable from simple arguments. For example, Q^{-1} estimates derived from the half-width of a resonance peak appear to be surprisingly accurate well into the nonlinear regime. Similarly, the nonlinear interaction of one-dimensional pulses does not lead to strong departures from linear superposition in the range of nonlinear behavior we have considered. On the other hand, the propagation of a one-dimensional narrow pulse through a medium with frequency-independent, but amplitude-dependent, Q is not described accurately by an equivalent Q operator.

Laboratory constraints

Seismic attenuation depends on a large number of conditions. These include pressure, temperature, porosity and saturation of the rock, and of course frequency and amplitude of the propagating wave. The bulk of laboratory evidence accumulated to date indicates that nonlinear processes are activated in rocks at strain levels above 10^{-6} [e.g. *Mavko*, 1979; *Johnston and Toksöz*, 1980; *Liu and Peselnick*, 1979; *Bulau et al.*, 1984]. *Stewart et al.* [1983] reviewed the available data and conducted additional experiments in which nonlinearity was shown to decrease markedly at confining pressures high enough to close many cracks. They explain the observations with a model where attenuation for dry rock at low to moderate confining pressure is caused by frictional work dissipation at crack asperities in Hertzian contact. For large strains, the attenuation increases linearly with strain amplitude and crack density, and decreases with confining pressure according to the relation:

$$Q^{-1} = Q_a^{-1} + k\zeta P^{-4/3} \epsilon \quad (1)$$

where k is a material constant, ζ is the crack density, ϵ is the strain amplitude, and P the confining pressure. Here Q_a^{-1} represents the linear attenuation controlled by anelastic mechanisms that mask the nonlinear ones at low strain. *Tittman* [1983] showed that a

similar amplitude dependence also holds for halite, both in the form of pressed salt and in dome salt.

The experimental and analytical methods used to measure Q in the laboratory fall generally in three main categories [e.g. *Nowick and Berry, 1972*]:

1. Quasi-static measurements, in which we can include hysteresis loop techniques, stress relaxation and creep recovery experiments.
2. Resonance experiments, in which a device with large external inertia is used to control the period of free or forced resonance of the system. This class includes torsion pendulum measurements and vibrating bar measurements.
3. Wave propagation experiments, which include both continuous wave and short pulse measurements.

A important issue for our present purposes is that the experimental setup and data reduction techniques used in many of these experiments are based on linear concepts. For instance, in one type of hysteresis loop measurements, the phase angle ϕ of stress-strain cycles is evaluated by signal analysis, and attenuation is measured by $Q^{-1} = \tan \phi$ which holds as long as the rheology is linear. Similarly, in forced resonance experiments, the half width $\Delta\omega$ of the "Lorentz" peak is used to define Q^{-1} at or near the resonance frequency ω_0 , by the relation $Q^{-1}(\omega_0) = \Delta\omega / \omega_0$. Again, this equation is derived by linear perturbation analysis of the resonant system, and holds in the low-loss case. In wave propagation experiments, typical approaches involve the calculation of spectral ratios of pulses propagated through the medium under study and through a high- Q reference medium. Another approach is to measure the increase in rise-time of a pulse as it is attenuated. Both methods rely implicitly on a linear analysis of pulse propagation. Of concern is the fact that most documented observations of amplitude-dependent Q rely on such techniques, and the relation (1), which clearly indicates nonlinear behavior, is actually fitted to observations derived from a linear analysis. It is therefore legitimate to raise the question of whether the interpretation of amplitude-dependent Q observations contains internal inconsistencies, and possible biases. Furthermore, whereas our intuition is usually a very good guide when it comes to gauging the effects of small perturbations in the linear regime, this is no longer the case when nonlinearities dominate. Consequently, it is not a foregone conclusion that the effects of nonlinear Q can be gauged with "back-of-the-envelope" arguments.

A notable exception to the concerns raised above consists of hysteresis loop experiments in which attenuation is defined by $Q^{-1} = \Delta E / 4\pi\langle E \rangle$ [e.g. *O'Connell and Budiansky, 1978*], where ΔE is the dissipated energy (measured by the loop area) and $\langle E \rangle$ the average stored energy in the course of a cycle. The definition of Q^{-1} does not

depend on the shape of the loop, which is elliptical in the linear regime and develops cusps when nonlinearity appears at large strains [e.g. *Brennan and Stacey, 1977; Liu and Peselnick, 1983*]. *Coyner and Martin [1990]* have recently shown that a correct interpretation of such hysteresis loops leads to Q^{-1} estimates for a variety of rock types which are quite consistent with estimates obtained by other techniques. This includes the monotonic increase of Q^{-1} with strain amplitude at strains greater than 10^{-6} . This consistency may be taken as a justification to accept published studies on nonlinear Q in spite of the use of linear data analysis.

In an attempt to identify possible pitfalls and to evaluate quantitatively the predicted effects of nonlinearity, we have conducted three groups of simple numerical experiments with one-dimensional linear and nonlinear systems of the type that can be described by equation (1). They are:

1. simulations of forced vibration of nonlinearly damped one-dimensional oscillators, to examine the distortion of Lorentzian peaks induced by nonlinearity,
2. tests of whether a pair of one-dimensional pulses propagating in opposite directions in a nonlinear medium superpose quasi-linearly,
3. comparison of the results of spectral ratio analysis and pulse shape interpretations (e.g. rise times) in both linear and nonlinear one-dimensional pulse propagation simulations.

Numerical experiments

Model formulation

To perform the suite of experiments described above, we use an attenuation model described by

$$Q^{-1} = Q_a^{-1} + \gamma \epsilon \quad , \quad (2)$$

where ϵ is the strain amplitude and γ is a material constant. This is a specialization of equation (1), which was introduced by *Mavko [1979]* and was subsequently used by *Minster and Day [1986]*.

For simulations of resonance experiments, we adopt a 3-parameter attenuation model characterized by a single relaxation mechanism for simplicity. This mechanism is selected to center the absorption band at the resonance frequency, so that the appropriate Q^{-1} value is that at the center of the absorption band. In that case the attenuation model is completely specified by ω_0 , the center frequency of the band, $Q_0^{-1} = Q^{-1}(\omega_0)$, the attenuation at the center of the band, and by a modulus or a wave velocity. In terms of a standard linear solid

model [e.g. *Nowick and Berry*, 1972; *Liu et al.*, 1976], the strain retardation and stress relaxation times are given by:

$$\tau_\epsilon = \omega_0^{-1} (\sqrt{Q_0^2 + 1} + Q_0^{-1}) \quad (3)$$

$$\tau_\sigma = \omega_0^{-1} (\sqrt{Q_0^2 + 1} - Q_0^{-1}) \quad (4)$$

Since we are interested in solving a quasi monochromatic problem, we can specify the phase velocity c_0 at the center frequency ω_0 as the third model parameter. The relaxed and unrelaxed moduli are then given by:

$$M_R = \frac{2\rho c_0^2}{1 + \tau_\epsilon/\tau_\sigma} ; M_U = \frac{2\rho c_0^2}{1 + \tau_\sigma/\tau_\epsilon} \quad (5)$$

Although this model entails a frequency dependence of Q^{-1} , with Q^{-1} increasing as ω at frequencies less than ω_0 , and decreasing as ω^{-1} at frequencies higher than ω_0 , the influence of frequency dependence is in fact negligible, because the width of the Debye peak (the absorption band) is much larger than that of the Lorentz peak (the resonance) in all calculations described below. In other words, Q^{-1} is essentially frequency-independent in the range covered by the calculations. To simulate nonlinearity, we simply make Q_0^{-1} depend linearly on the strain amplitude of the oscillations.

For pulse propagation experiments, we use the Padé approximant method described by *Day and Minster* [1984], slightly modified to include poles at zero and infinite frequency, as described by *Day and Minster* [1990]. This allows us to use a broad absorption band (that is, broader than the frequency band covered by the finite-difference algorithm), and to specify the attenuation properties in each cell at each time step independently, based on the current strain amplitude. This remedies the noncausal character of the calculations performed by *Minster and Day* [1986].

Resonance experiment

In resonant bar experiments, amplitude is obtained as a function of frequency near a normal mode of the sample. (The frequency of this mode is typically adjusted by addition of large external inertia.) The amplitude and width of the resulting "Lorentzian" peak are controlled by the attenuation – larger attenuation leads to a lower, broader peak. For linear attenuation in which the width of the resonance peak is relatively narrow (e.g. $Q^{-1} < \sim 0.1$), the resonance peak is essentially symmetric (Figure 1a) and Q can be obtained simply from the width of the peak at the half-power level, $Q^{-1} = (\omega_2 - \omega_1)/\omega_r$. In the case of amplitude-

dependent attenuation, the peak becomes distorted and is steeper on the lower frequency side (see Figure 1b). A simple argument to explain this distortion invokes the effect of the amplitude dependence on the phase velocity: the larger amplitude, and thus larger attenuation, near the top of the peak causes a reduction in the phase velocity and a corresponding shift of the resonance to lower frequencies. However the sides of the peak are not shifted, because the oscillations have low amplitudes at those frequencies, so the overall peak shape is asymmetric and skewed to the left.

Figure 2 shows examples of distorted Lorentz peaks obtained from high-strain flexure experiments in salt (data from *Bulau et al.*, 1985). Despite the often considerable asymmetry in the peak shapes, experimenters typically continue to estimate Q^{-1} by measuring the peak width at the half-power level. In order to test for possible biases introduced by this practice, we computed synthetic Lorentzian peaks through numerical simulations of a harmonic oscillator with nonlinear attenuation. We use a simple finite difference scheme and, as described earlier, take attenuation to be of the form (2). When these simulations are performed for constant γ , but increasing forcing amplitude, the Lorentzian peaks become distorted and are indeed skewed to the left (Figure 3). However, when we calculate Q^{-1} from these peaks using the expression $Q^{-1} = (\omega_2 - \omega_1)/\omega_r$ and ignoring the peak asymmetry, the resulting values of Q^{-1} vary linearly with the maximum strain amplitude ϵ_{max} (Figure 4). The slope γ computed from these Q estimates is reasonably close to the γ actually used in the simulations. In other words, application of the linear concept yields the "correct" answer to an acceptable approximation. We conclude therefore that Q measurements based on the half-width of distorted Lorentzian peaks probably give reasonably correct results, even well into the nonlinear regime.

In principle, it might be possible to recover the amplitude dependence of Q^{-1} (e.g. γ) from a single Lorentz peak measurement by measuring the distortion of the peak. In order to test this possibility, we considered a skewness parameter defined as $s = (\omega_2 - \omega_r)/(\omega_r - \omega_1)$. In our synthetic experiments, s increased with increasing strain but seemed to saturate at about $s=1.5$. In contrast, the Lorentz peaks from the laboratory salt experiments (Figure 2) were more severely distorted with values of s up to 2 or higher. Thus, our simulations were not completely successful in reproducing the shapes of some of the observed Lorentz curves. This may reflect a limitation in our modeling procedure, or, alternatively, may indicate that the attenuation in the laboratory experiments cannot be modeled as a simple linear function of strain amplitude. In spite of this caveat, we conclude that resonant-bar laboratory measurements of amplitude dependence of Q^{-1} are in fact a fairly accurate characterization of the nonlinear material properties.

Pulse superposition experiment

The pulse superposition numerical experiments were motivated by results from some small-scale laboratory experiments performed by *Larson* [1982]. The laboratory experiments were intended to test whether linear superposition applied to the propagation of pulses with maximum strain of about 7×10^{-4} . At this strain level, substantial departure from linear superposition would be expected. In the laboratory experiments, two nearly identical explosive sources were simultaneously detonated approximately 10 cm apart in pressed salt, and the velocity waveforms were recorded along the plane of symmetry between the sources. These velocity recordings were obtained at a source-receiver distance comparable to the separation distance between the two sources. The resulting velocity records from the combined explosions were in each case in very close agreement with the sum of the velocity records from the individual charges.

The above result was interpreted as evidence for the applicability of linear superposition in wave propagation in salt at relatively high strains. This is in apparent contradiction to other laboratory measurements in the same material, which consistently show evidence of amplitude-dependent losses at comparable strain levels. An alternative interpretation, which we examine in this section, is that an experiment of this type is simply not sensitive to deviations from linearity.

To address this issue, we describe a series of numerical simulations of pulse propagation. The numerical experiments are for plane waves in a simple nonlinear rheology which nevertheless mimics the laboratory-observed amplitude dependence of Q as summarized earlier.

The model for nonlinear attenuation is constructed in two steps. First, we use the Padé approximant method of *Day and Minster* [1984, 1990] to convert the stress-strain relation of a linear, anelastic solid, with frequency-independent Q , into differential form. *Minster* [1978a] shows that an absorption band, with Q nearly constant at Q_0 , and with minimum and maximum relaxation times τ_1 and τ_2 , respectively, yields the following relation between stress history, $\sigma(t)$ and strain history, $\epsilon(t)$

$$\sigma(t) = \int_0^t M_u \left[1 - \frac{2}{\pi Q_0} \int_{\tau_1}^{\tau_2} \left(1 - e^{-(t-t')/\tau} \right) \frac{d\tau}{\tau} \right] d\epsilon(t') , \quad (6)$$

where M_u is the unrelaxed modulus. Day and Minster show that (6) can be approximated by

$$\sigma(t) = M_u \left[\epsilon(t) - \sum_{i=1}^n \zeta_i(t) \right], \quad (7)$$

where the ζ_i 's are relaxation terms governed by the n linear equations

$$\frac{d\zeta_i}{dt} + v_i \zeta_i = \frac{\tau_1^{-1} - \tau_2^{-1}}{\pi} w_i Q_0^{-1} \epsilon(t), \quad (8)$$

The constants v_i and w_i which depend on the order of approximation, n , are given by Day and Minster [1984, 1990], who also show that the operator defined by (7) and (8) converges to the exact result (6) as n increases.

The second step is to generalize (8) by introducing a linear dependence of Q_0 on strain amplitude according to (2):

$$\frac{d\zeta_i}{dt} + v_i \zeta_i = \frac{\tau_1^{-1} - \tau_2^{-1}}{\pi} w_i (Q_u^{-1} + \gamma \epsilon(t)) \epsilon(t). \quad (9)$$

Then, (7) and (9) constitute the stress-strain equations for our set of one-dimensional finite difference simulations.

The source is a velocity pulse—in agreement with Larson's experiments—with time history

$$v(t) = \begin{cases} 0.5 [1 - \cos(2\pi t/T)], & 0 < t < T \\ 0, & t < 0 \text{ or } t > T \end{cases}, \quad (10)$$

introduced at a plane boundary. Figure 5 shows the velocity time histories at 5 different distances from the source, for a calculation in which Q_u is 1000 and the product of γ and the maximum strain at the source is equal to 0.3. In other words, the amplitude dependence is such that Q assumes a minimum value of about 3 near the source. As a result of the very low effective values of Q , the plane wave amplitude attenuates rapidly with distance of propagation. Furthermore, the amplitude dependence of the attenuation causes the pulse to evolve into a distinctive shape, with an initial steep rise, followed by a more gradual slope. The break in slope is not present for the linear attenuation model (i.e., $\gamma = 0$). As in the case of the distorted Lorentz peaks, we can offer a simple explanation for

this peculiar pulse shape: the crest of the pulse has large amplitude and is thus associated with low Q , and therefore low phase velocity. Consequently, the crest of the wave gets progressively delayed with respect to both the low amplitude onset and tail of the pulse.

Figure 6 shows the corresponding time histories when two plane waves traveling in opposite directions interact. In this case, identical velocity pulses of form (10) were introduced simultaneously, separated by 20 times the initial pulse width (travel time separation of $20T$). Figure 7a compares the two-source waveform, at the midpoint, with twice the single-source waveform. This is the one-dimensional analogue of Larson's laboratory superposition experiment. As in the laboratory experiment, the numerical experiment shows near-perfect agreement. Finally, Figure 7b compares the two-source waveforms, after pulse interaction is completed, with the single-source waveform. Again, agreement is very close: although the effect of imperfect superposition is visible in the theoretical calculation, it is small enough that it would be masked by experimental uncertainties. Comparable results were obtained in this comparison when destructive, rather than constructive, interference between the sources was present in the numerical experiment.

These results show that this type of experimental observation is not diagnostic of deviations from linearity. This insensitivity apparently results because the pulses superpose only briefly as they cross. For the amplitude-dependent relaxation model, this brief interaction is insufficient to discernibly perturb the individual source pulses. This is so even though the individual pulses themselves have been substantially modified as a result of the nonlinearity of the model.

Spectral ratios

One of the standard methods for estimating Q from seismic observations is the spectral ratio method. For amplitude-independent attenuation, the spectral attenuation of a plane wave is exponential in the frequency, f , and propagation distance x ,

$$\bar{v}(f, x) = e^{-\pi f x / c Q}, \quad (11)$$

where c is the wave speed. Then, if we assume that Q is approximately frequency-independent, the logarithm of the spectral ratio of observations at distances x_1 and x_2 is linear in the frequency f :

$$\log_{10} \left(\frac{v_2}{v_1} \right) = -\frac{\pi}{\ln 10} \frac{x_2 - x_1}{c Q} f. \quad (12)$$

The Padé approximant method reproduces this behavior of frequency- and amplitude-independent Q models, as shown by *Day and Minster* [1990]. In this section, we examine the effect of amplitude dependent Q on spectral ratio measurements of plane waves. Numerical experiments are performed using a displacement—rather than velocity—source pulse of form (10). One complication which we examine in particular results directly from the introduction of nonlinearity, and concerns the possibility of energy transfer from one frequency component to another.

For comparison purposes, and as verification of the numerical method, we present results for a linear (amplitude-independent Q) calculation, with Q equal to 20, in Figures 8 and 9. Figure 8 shows displacement time histories at distances of 4, 12, and 20 times the source pulse width (i.e., $4cT$, $12cT$, and $20cT$). Figure 9 shows the corresponding spectra divided by the source spectrum. Note that, over most of the frequency range plotted, the spectral ratios follow the log-linear relationship of Equation 12, as expected. Also note that all spectral ratios approach unity in the low-frequency limit, to very high accuracy. This agrees with the usual “linear” reasoning that when the wavelength exceeds the propagation distance, then attenuation has little chance to affect spectral amplitudes.

Figure 10 shows time-domain displacements for a nonlinear calculation, with Q_a equal to 1000 and the product $[\gamma \times \epsilon_{\max}]$ equal to 0.3, i. e., $Q_{\min} \approx 3$. The most notable difference between these time-histories and those for the linear case is that the tail of the pulse is of shorter duration in the nonlinear case, making the pulse more symmetric in appearance.

The spectral ratios given in Figure 11 show a substantial deviation from the linear case, however. The most important difference is that the spectral ratios in this case do not approach 1 at zero frequency. At a distance of $4cT$, the zero-frequency spectral value is only half of its value for the source pulse, and the zero-frequency spectrum continues to diminish by a further 15% as distance increases to $20cT$. Furthermore, at least in some cases, the attenuated spectra have a slight peak, which means that the pulse does not remain unipolar as it propagates, a phenomenon which can be detected in the pulse shapes shown on Figure 8. This low-frequency behavior is a nonlinear phenomenon which has no counterpart in the linear case.

The other distinction between spectral ratios for the linear and nonlinear cases is the increasing slope in the nonlinear case above a frequency of about $1/T$. This is a consequence of the amplitude dependence of the attenuation mechanism. High frequencies associated with the discontinuous acceleration at the onset of the displacement pulse are relatively less attenuated in the nonlinear case, because the pulse onset is associated with relatively small strain amplitudes. The spectral ratios for the nonlinear case are further

distorted as the frequency approaches $2/T$, as a result of energy transfer from one frequency band to another. The source spectrum has a null at $2/T$, and nonlinearity causes a small amount of energy leakage into this band. While the effect is relatively small, the presence of a null in the source spectrum results in a large effect on the spectral ratios in the vicinity of $2/T$. As with the low-frequency behavior, these high-frequency phenomena have no counterpart in the case of linear attenuation models.

For nonlinear simulations with somewhat smaller values of γ , similar phenomena occur, but are correspondingly less pronounced. For $[\gamma \times \epsilon_{\max}]$ equal to 0.1 ($Q_{\min} \approx 10$), for example, the zero-frequency spectral ratio is about 0.8 at a distance of $20cT$.

The numerical experiments also provide evidence that the behavior of the low-frequency spectral components is likely to be sensitive to the shape of the source pulse. For example, simulations verify that a unipolar *velocity* pulse propagates in the present model *without* reduction of the zero-frequency spectral component, in contrast to the above results for a unipolar displacement pulse. In other words, in the nonlinear model, integration does not commute with the attenuation operator, as must be the case for all linearly anelastic models. This means in particular that nonlinear pulse propagation characteristics depend on the shape (i.e. the spectral content) of the pulse itself.

Yet another method for estimating Q^{-1} from pulse propagation experiments is to map directly the rise time of the pulse into attenuation estimates through:

$$\tau_r = \tau_r^0 + C t_u Q^{-1} \quad (13)$$

where τ_r is the rise time of the attenuated pulse, τ_r^0 the rise time of the input pulse, and t_u is the (unrelaxed) travel time. Here C is a constant equal to approximately 0.5, as shown by several authors [e.g. Gladwin and Stacey, 1974; Minster, 1978b; Kjartansson, 1979]. Stewart *et al.* [1983] used the technique in high-strain experiments to demonstrate amplitude dependence of Q^{-1} in dry Berea sandstone. The pulses shown in Figures 5 and 6 illustrate the problem we have in verifying this relation for the nonlinear case. Because of the peculiar distortion of the pulse, the rise time is not easily defined using the tangent at the inflection point as defined by Minster [1978b]. Further, for linear mechanisms, not only the rise time, but all time scales within the pulse scale with a certain power of $t_u Q^{-1}$ as shown by Minster and Vassiliou [1979] and Minster [1980] (The exponent depends on the frequency dependence of Q). It is easy to verify that these simple scaling laws are not obeyed by the pulses shown here, which raises the question of how the high-strain laboratory data should be interpreted. It is possible, however, that scaling laws might be

obeyed reasonably well by pulses with a different shape, more similar to those generated in the laboratory experiments.

Discussion

An issue of some importance is that although the algorithms satisfy the basic laws of continuum mechanics, it is not guaranteed that they simulate the rheology of any real material. The application of amplitude-dependent properties in a completely local mode — both in space and in time — remedies objections raised to the treatment of the same problem by *Minster and Day* [1986]. However, the drop in displacement pulse spectral amplitudes at DC is somewhat counter-intuitive, intriguing, and peculiar to the nonlinear regime. This behavior is quite different from that of the classical linear “*Q* operator”, which preserves the area under a unipolar displacement pulse as it propagates and attenuates. The nonlinear calculation does not preserve this area, nor does it preserve unipolarity. This caused us to become concerned about the application of the boundary condition at one end of the one-dimensional medium. A finite-duration force applied to a boundary would immediately produce a displacement pulse with a tail which, strictly speaking, is of infinite duration (i.e., decays asymptotically to zero). In other words, we introduce a finite-duration pulse in a medium that is incapable of supporting one, which is true even in a linearly anelastic medium. Thus, our finite-duration displacement pulse implies a forcing function of infinite duration, and rather artificially shaped to suppress the late-time displacement at the source. While the spectral ratios for a linear *Q* model are insensitive to the nature of the forcing, in a nonlinear model they will depend on its time-history and amplitude. There exists therefore a possibility that, in the nonlinear case, the boundary condition interacts with the outgoing pulse in a way that could affect the spectral analysis. This is intimately related to the issue that the propagation is pulse-shape dependent, so that use of an artificial input pulse could cause strange results.

As a check, we constructed a composite one-dimensional medium by adjoining a linear elastic section to the nonlinear one. A displacement pulse of the form (9) was then created in the elastic section, and the total linear momentum in the system calculated at a time when the trailing edge of this pulse was clearly detached from the boundary, but its leading edge had not yet reached the nonlinear section. At this time, no more work was performed by the boundary condition, and the end node could be left free. At the interface between the elastic and nonlinear media, this incident pulse generates both a reflected and a transmitted pulse, and the transmitted pulse was attenuated as described previously, in a way that preserved the total momentum in the system. This is an indication that the simulations are

dynamically correct, but it says little about the thermodynamics of the system, other than it is clearly lossy.

At first glance, a somewhat surprising aspect of field observations is that linear attenuation models should perform reasonably well in explaining data which we feel certain to be contaminated by nonlinear effects. This is true, for example, of the SALMON data modeled by *McCartor and Wortman* [1985, 1989], of the COWBOY data used by *Minster and Day* [1986], and of the laboratory data for pressed salt collected by *Larson* [1982]. We feel that a plausible reason is that the main effect to be explained is the combination of pulse broadening and amplitude decay with increasing distance: linear Q models offer enough flexibility to accommodate a fairly wide range of observations, provided that one is willing to choose rather extreme models (e.g. $Q^{-1} \geq 0.1$ in the nonlinear zone). On the other hand, a straightforward spectral analysis—a linear technique—of SALMON near-field data led *McCartor and Wortman* [1989] to the conclusion that effective Q is anomalously low at low frequencies, in qualitative agreement with our results on low-frequency spectral ratios. However, since such Q values are much smaller than the typical laboratory values measured on the same rocks, the physical meaning of these models is questionable. In fact, in cases of extreme attenuation, it is debatable whether the concept of Q is useful in the first place. In the case of data collected within the “elastic radius”—such as the SALMON data—the physical explanation offered by *Sammis* [1989] which ascribes the pulse broadening to damage mechanics, as developed by *Ashby and Sammis* [1989], seems a good candidate. In particular, it incorporates scale effects explaining why comparable pulse-broadening is not seen in small-scale explosions in dry rock [e.g. *Nagy and Florence*, 1986, 1987, 1988]. On the other hand, whether this explanation, primarily intended for granite, is also appropriate for salt is open to question.

As we have seen (see Figure 7), the puzzling fact that *Larson* [1982] observed apparent linear superposability of pulses in salt with peak strains in excess of 10^{-4} is not so surprising after all. This superposability test is simply too weak a test of linearity. As argued by *Savage and Hasegawa* [1967], a more general test of linear superposition, and thus of linearity, would be achieved by comparing the attenuation of both sinusoidal and non-sinusoidal disturbances in the spectral domain. (They used this technique to reject the variable-friction mechanism originally proposed by *Knopoff and MacDonald* [1958] as a candidate for attenuation of low amplitude seismic waves.) This technique might be adapted to our present problem by comparing spectral decays from free vibrations of a test bar in the laboratory [e.g. *Bulau et al.*, 1985], with those estimated from travelling pulses as measured in *Larson's* [1982] experiments. In point of fact, the forced resonance curves

measured by Tittman and his co-workers in essentially the same material, are increasingly distorted as strains increase beyond 10^{-6} , a clear indication of nonlinearity.

Implications for explosion sources

In order to achieve any sort of predictive capability concerning coupling and coupling variability of underground explosions, one must be capable of constructing numerical models that simulate the expected radiation field under various hypotheses. Considerable research and development has been targeted at this problem over the past 30 years, and models have reached a remarkable level of sophistication [see for example, *Cherry et al.*, 1975; *Bache*, 1982; *Cherry and Rimer*, 1982; *Day et al.*, 1983]. Most of this effort has been aimed at modeling accurately the regime prevalent immediately around the cavity, where extreme nonlinear damage takes place because the loading path crosses the yield surface. As noted earlier, some controversial aspects remain, particularly concerning the effect of dilatancy [e.g. *Nikolayevskiy et al.*, 1978; *Cherry and Rimer*, 1982; *Bache*, 1982; *Scholz*, 1982]. The potential implications of the simulations described in the previous section for the characterization of explosion sources are several. We shall summarize them in this section.

If we assume that $Y^{-1/3}$ scaling with yield holds [e.g. *Trulio*, 1978; *Larson*, 1982], nonlinear rheology may well prevail to scaled slant ranges as large as 10^2 - 10^3 $\text{mkg}^{-1/3}$ [e.g. *Minster and Day*, 1986]. In contrast, numerical models of explosive sources usually assume the rheology to be linear beyond the so-called "elastic" radius, where the stress-strain path followed by material particles ceases to intersect the assumed yield curve; this may happen at strains as large as 10^{-4} [e.g. *Cherry et al.* 1975; *Cherry and Rimer*, 1982]. Therefore, there has to exist a domain surrounding the explosion, where the peak strains are not so large as to cause failure of the medium, but large enough to trigger nonlinear attenuation mechanisms. This conclusion was reached by *Minster and Day* [1986] and is not invalidated by our present results.

In cavity-decoupling scenarios, complete decoupling is defined by the condition that the cavity wall is not subjected to stresses high enough to cause it to yield [e.g. *Larson*, 1985]. However, this definition does not preclude loads high enough to cause nonlinear attenuation. In fact, if complete decoupling were defined in terms of truly linear behavior of the cavity wall, then it would require such large cavities as to be impractical [e.g. *Archambeau*, 1985]. These issues are discussed in detail in the proceedings of the June, 1985 DOE workshop held in Pajaro Dunes, California [*Larson*, 1985]. An important issue, from the point of view of source theory is whether this has a significant effect on observable teleseismic waves, and particularly on coupling in the 1 Hz band, since this is

what controls magnitude estimates. Some of the results presented here indicate that this might indeed be the case, but because the solution to one nonlinear problem cannot be safely applied to another problem, there remains an uncomfortable margin for uncertainty.

We have therefore clear reason to think that we observe the seismic source through a screen consisting of a nonlinear zone in the immediate vicinity of the source. If Q^{-1} increases very strongly with increasing amplitude, (i.e. the medium is strongly nonlinear), then we should expect amplitudes to decrease very rapidly with range close to the source, and drop to linear levels almost immediately. On the other hand, in the case of mild nonlinearity, high amplitudes will persist to larger ranges, being controlled predominantly by geometrical spreading, and the size of the nonlinear zone could be much larger. In the former case, intuition would indicate that the dimension of the nonlinear attenuating zone is much smaller than teleseismic wavelengths, so that teleseismic waves might not be affected very much; in the latter case, the converse might be true. Unfortunately, the disquieting result shown on Figure 11 is that nonlinear rheology can affect the spectral content of a source pulse at all wavelengths. This means that even a small nonlinear zone—say, a fraction of a wavelength thick—has the potential to affect significantly the effective source spectrum at teleseismic frequencies of interest. In particular, we cannot rule out the possibility that body wave magnitudes (and therefore yield estimates) might be affected for all explosions, large and small. To complicate matters, if the relevant physical mechanism is indeed due to friction between crack surfaces in the rock, then one should have to account for differences in attenuation above and below the explosion, due to the differences in confining pressure; this suggests that if nonlinear attenuation is important at all, spherically symmetric models will not suffice to describe its effects on the far field radiation.

On the other hand, we view such intuitive arguments with considerable caution when nonlinearities play a role. In particular, we must emphasize that quantitative results obtained from one-dimensional simulations cannot be used to infer quantitative conclusions for even the simplest (spherically symmetric) three-dimensional case. This is because geometrical spreading cannot be accounted for after the fact, but must be introduced in the heart of the calculation, where it does not commute with attenuation. Furthermore, we have noted that the spectral ratio results shown in Figure 11 are pulse-shape dependent. This means that, except in a qualitative sense, firm conclusions concerning the impact of nonlinear attenuation on the effective source will require true three-dimensional simulations using a realistic source function.

One constraint on any nonlinear rheological model, as discussed by *Minster and Day* [1986] and also by *Trulio* [1985], is that it must not violate the empirically verified yield

scaling laws. Only rate-independent rheologies will not destroy scaling, and even a linear Q model, *sensu stricto*, does introduce a rate-dependence through the physical dispersion required to satisfy causality. This means that large explosions which generate a wavefield considerably enriched in low frequencies relative to small ones, "see" a slightly different medium after the $Y^{-1/3}$ scaling is applied. In practice, the main reason why a linear Q model, even with extremely low Q values, does not invalidate the scaling laws is that the physical dispersion associated with attenuation is not severe. Since our calculations show that the characteristics of nonlinear pulse propagation are pulse-shape sensitive, a special set of three-dimensional simulations will be required to verify the scaling is preserved.

On the other hand, *Murphy* [1989, personal communication] points out that observed teleseismic moment estimates for nuclear explosions are in quite good agreement with those expected on the basis of cavity dimensions. This should not be the case if nonlinear effects are significant. This comment has considerable merit, but is not necessarily in direct conflict with the results presented above. The one-dimensional simulations do not deal at all with near-field effects, and only show that the final (static) displacement field—including the final cavity size—is reached according to a history (time function) that depends on range in a more complicated way than we typically assume, and is affected by the local nonlinear rheology. Strictly speaking, the moment is not affected. On the other side of the issue, *Evernden et al.* [1986] argue that the equivalent elastic radii inferred from teleseismic corner frequency measurements for many explosions in different media are larger than those predicted from finite difference models adjusted to fit near-field observations [e.g. *Rimer and Cherry*, 1982]. Further, these authors used a very simple source representation due to *Sharpe* [1942], in which a step function pressure of amplitude P_0 is applied at an elastic radius R_0 , where P_0 should be comparable to the effective compressional strength of the material. They conclude that values of P_0 required to fit the data fall well below the rock strengths used in the numerical models, and the values of R_0 are larger than the numerical "elastic" radius. This may suggest either unsuspected weakness of the surrounding material near explosions detonated at NTS and other U.S. sites, or unmodeled nonlinear behavior extending to larger distances from the source.

Conclusions

Because most rocks exhibit nonlinear amplitude-dependent attenuation at moderate to high strains and relatively low confining pressure, the transition to the elastic regime in the vicinity of an underground explosion involves a nonlinear zone separating the classical "elastic radius" from the truly linear (anelastic) far-field regime. Modeling the wavefield within that zone is difficult because we cannot use the usual mathematical techniques

which, for the most part, depend on the principle of superposition, and therefore on the assumption of linearity.

The simple numerical experiments described in this paper lead us to one major conclusion, namely that the effects of nonlinear attenuation on wave propagation are not easily predicted by simple arguments, even after simulation. In some instances of interest, such as the evaluation of Q^{-1} from Lorentz peaks, nonlinearity seems to have only a modest effect. Similarly, some departures from linear pulse superposition are not very severe. On the other hand, the results demonstrably depend on the initial pulse shape, so that it is necessary to assess each problem through a separate calculation using the correct geometry and the right pulse shape. It is a measure of our lack of reliable insight into this class of nonlinear wave propagation problems that even the simplest simulations are not easily interpreted, and that the inferences one can attempt to draw concerning more realistic situations remain somewhat tentative.

Acknowledgments

This research was supported by the Defense Advanced Research Projects Agency under Geophysics Laboratory contract No. F19628-88-K-0039. We are grateful to J. Bulau and B. Tittman for providing us with the original resonance curves depicted on Figure 2. We thank Dr. Steven Taylor of the Lawrence Livermore National Laboratory for his patience and his encouragement to prepare this report.

References

- Archambeau, C.B., Comments on nonlinear strain-dependent losses in the near-source region of (coupled and decoupled) explosions, in: *Proceedings of the Dept. of Energy sponsored cavity decoupling workshop* Pajaro Dunes, CA, July 29-31, 1985, D.B. Larson, ed., 1985.
- Ashby, M.F., and C.G. Sammis, The damage mechanics of brittle solids in compression, *Pageoph*, **133**, 489-521, 1990.
- Bache, T.C., Estimating the yield of underground nuclear explosions, *Bull. Seimol. Soc. Amer.*, **72**, S131-S168, 1982.
- Brennan, B.J., and F.D. Stacey, Frequency dependence of elasticity of rock-test of seismic velocity dispersion, *Nature*, 268, **220-222**, 1977.
- Bulau, J.R., B. R. Tittman, M. Abdel-Gawad, and C. Salvadó, The role of aqueous fluids in the internal friction of rock, *J. Geophys. Res.*, **89**, pp. 4207-4212, 1984.
- Bulau, J.R., B.R. Tittman, and M. Abdel-Gawad, Nonlinear wave propagation in rock, *I.E.E.E. Trans.*, 1985.
- Cherry, J.T., N. Rimer, and W.O. Wray, Seismic coupling from a nuclear explosion: the dependence of the reduced displacement potential on the nonlinear behavior of near source rock environment, *S-Cubed rept. SSS-R-76-2742*, S-Cubed, La Jolla, CA, 1975
- Cherry, J.T., and N. Rimer, Verification of the effective stress and air void porosity constitutive models, *S-Cubed rept. SSS-R-82-5610*, S-Cubed, La Jolla, CA, 1982
- Coyner, K.B., and R.J. Martin, III, Frequency dependent attenuation in rocks, *New England research Final Report*, Hanscom AFB, GL report No. GL-TR-90-0012, ADA222185, 1990.
- Day, S.M., N. Rimer, and J.T. Cherry, Surface waves from underground explosions with spall: Analysis of elastic and nonlinear source models, *Bull. Seismol. Soc. Amer.*, **73**, 247-264, 1983.

- Day, S.M. and J.B. Minster, Numerical simulation of attenuated wavefields using a Padé approximant method, *Geophys. J. R. Astr. Soc.*, **78**, pp. 105-118, 1984.
- Day, S.M. and J.B. Minster, Padé approximant method for broad relaxation spectra, *Geophys. J. Int.*, (submitted) 1990.
- Evernden, J., C. Archambeau, and E. Cranswick, An evaluation of seismic decoupling and underground nuclear test monitoring using high-frequency data, *Rev. of Geophys.*, **24**, 143-215, 1986.
- Gladwin, M.T., and M.D. Stacey, Anelastic degradation of acoustic pulses in rock, *Phys. Earth Planet. Int.*, **8**, 332-336, 1974.
- Johnston, D.H. and M.N. Toksöz, Thermal cracking and amplitude dependent attenuation, *J. Geophys. Res.*, **85**, pp. 937-942, 1980.
- Kjartansson, E., Constant- Q wave propagation and attenuation, *J. Geophys. Res.*, **84**, 4737-4748, 1979.
- Knopoff, L. and G. J.F. MacDonald, Attenuation of small amplitude stress waves in solids, *Rev. Mod. Physics*, **30**, pp. 1178-1192, 1958.
- Larson, D.B., Inelastic wave propagation in sodium chloride, *Bull. Seismol. Soc. Amer.*, **72**, pp. 2107-2130, 1982.
- Larson, D.B., *Proceedings of the Dept. of Energy sponsored cavity decoupling workshop* Pajaro Dunes, CA, July 29-31, 1985, D.B. Larson, ed., 1985.
- Liu, H.P. and L. Peselnick, Mechanical hysteresis loops of an anelastic solid and the determination of rock attenuation properties, *Geophys. Res. Letters*, **6**, pp. 545-548, 1979.
- Liu, H.P., D.L. Anderson and H. Kanamori, Velocity dispersion due to anelasticity: Implications for seismology and mantle composition, *Geophys. J. R. Astron. Soc.*, **47**, 41-58, 1976.
- Mavko, G.M., Frictional attenuation: an inherent amplitude dependence, *J. Geophys. Res.*, **84**, pp. 4769-4775, 1979.

- McCartor, G. and W. Wortman, Experimental and analytical characterization of nonlinear seismic attenuation, *Final report, Mission Research Corp. Rept. No. GL-TR-89-0282*, ADA219367, 1985.
- McCartor, G. and W. Wortman, Analysis of Salmon Near-field data for nonlinear attenuation, *Final report, Mission Research Corp. Rept. No. MRC-R- 900*, Geophysics Lab., Air Force Systems Command, 1989.
- Minster, J.B., Transient and impulse responses of a one-dimensional linearly attenuating medium, Part I: Analytical results, *Geophys. J. R. Astr. Soc.*, **52**, pp. 479-502, 1978a.
- Minster, J.B., Transient and impulse responses of a one-dimensional linearly attenuating medium, Part II: A parametric study, *Geophys. J. R. Astr. Soc.*, **52**, pp. 503-524, 1978b.
- Minster, J.B., Anelasticity and attenuation, in *Physics of the Earth's Interior*, ed. A.M. Dziewonski and E. Boschi, pp. 151-212, *Proceedings of the International School of Physics "Enrico Fermi"*, North Holland, Amsterdam, 1980.
- Minster, J.B. and S.M. Day, Decay of wavefields near an explosive source due to high-strain, nonlinear attenuation, *J. Geophys. Res.*, **91**, pp. 2113-2122, 1986.
- Minster, J.B. and M.S. Vassiliou, Pulse propagation in a frequency-dependent linearly attenuating medium, *Stanford Univ. Publ. Geol. Sci. I, XVII*, p. 64, Conference on Seismic Wave Attenuation, 1979
- Nagy, G. and A.L. Florence, Laboratory investigations of containment of underground explosions, *SRI Technical Rept. DNA-TR-86-271*, July 1986
- Nagy, G. and A.L. Florence, Spherical wave propagation in low-porosity brittle rocks, *SRI Technical Rept. under DARPA contract 9168505, SRI project PYC-2336*, April 1987
- Nagy, G. and A.L. Florence, Dynamic stress measurement in geologic materials and simulants in small scale laboratory experiments, *SRI preprint*, 1988

- Nikolayevskiy, V.N., A.N. Polyanichev, Ye.V. Sumin, and N.G. Yakubovich, Dilatation effects in an underground explosion, *Doklady Akademii Nauk SSSR*, **250**, 66-70, 1978 (1980 translation)
- Nowick, A.S. and B.S. Berry, *Anelastic Relaxation in Crystalline Solids*, 677 p., Academic Press, New York, 1972.
- O'Connell, R.J., and B. Budiansky, Measures of dissipation in viscoelastic media, *Geophys. Res. Lett.*, **5**, 5-8, 1978.
- Rimer, N. and J. T. Cherry, Ground motion predictions for the Grand Saline Experiment, S-CUBED topical report, *Vela Seismological Center Rept. No. VSC-TR-82-25*, 1982.
- Sammis, C.G., Seismic pulse broadening associated with fracture damage caused by explosions in crystalline rock, *Final report*, Geophysics Laboratory, Air Force System Command, Rept. No. GL-TR-89-0161, ADA261135, 1989.
- Savage, J.C., and H.S. Hasegawa, Evidence for a linear attenuation mechanism, *Geophysics*, **32**, pp. 1003-1014, 1967.
- Scholz, C.H., Rock strength under confined shock conditions, *Final technical report, S-Cubed rept. SSS-R-83-5906, to AFOSR*, October 1982.
- Sharpe, J.A., The production of elastic waves by explosion pressures, I. Theory and empirical observations, *Geophysics*, **7**, 144-154, 1942.
- Stewart, R.R., M.N. Toksöz, and A. Timur, Strain dependent attenuation: Observations and a proposed mechanism, *J. Geophys. Res.*, **88**, pp. 546-554, 1983.
- Tittman, B.R., Studies of absorption in salt, *Rockwell International Science Center Rept. No. SC5320.5FR*, 1983.
- Trulio, J.G., Simple scaling and nuclear monitoring, *Applied Theory, Inc. Rept. No. ATR-77-45-2a*, Los Angeles, Calif., 1978.
- Trulio, J.G., in: Proceedings of the Dept. of Energy sponsored cavity decoupling workshop Pajaro Dunes, CA, July 29-31, 1985, 1985.

Walsh, J.B. Seismic attenuation in rock due to friction, *J. Geophys. Res.*, **71**, 2591-2599, 1966.

Witte, D.C., *The Pseudo-spectral Method for Simulating Wave Propagation*, Ph.D. Thesis, Lamont-Doherty Geological Observatory, Columbia University, NY, 1989.

Witte, D.C., and P. Richards, The pseudo-spectral method for simulating wave propagation, *Proc. 2nd IMACS Symp.*, Intern. Assoc. Math. & Comput. in Simulation, 1990.

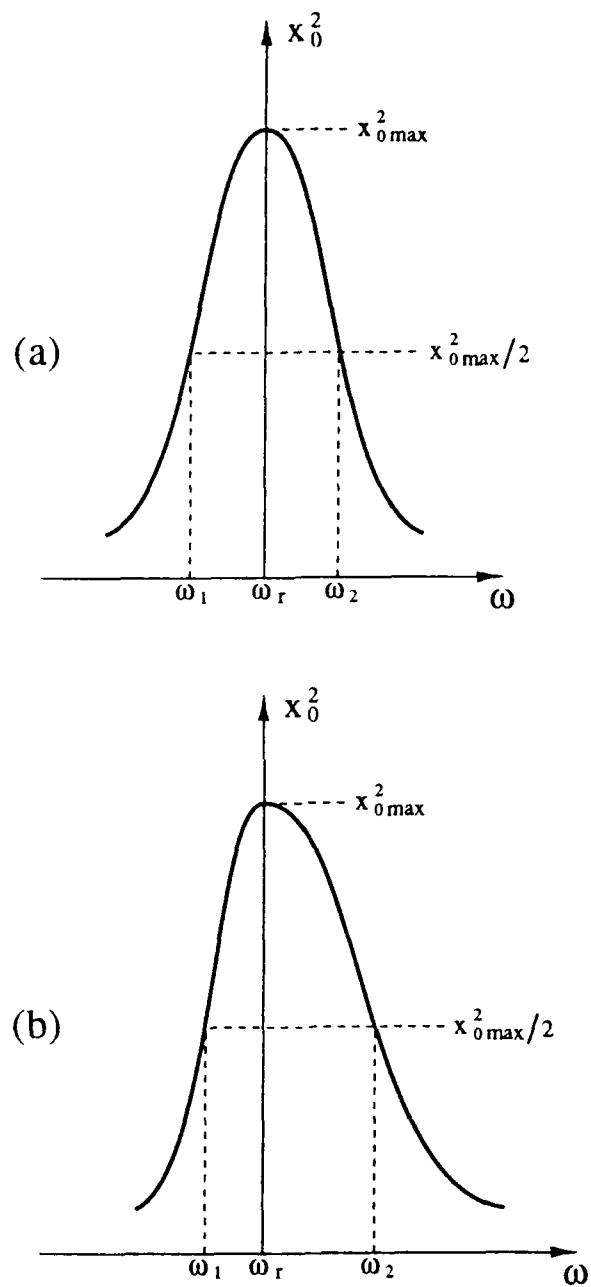


Fig.1. The shape of the Lorentz peak for: (a) linear attenuation, and (b) amplitude dependent attenuation.

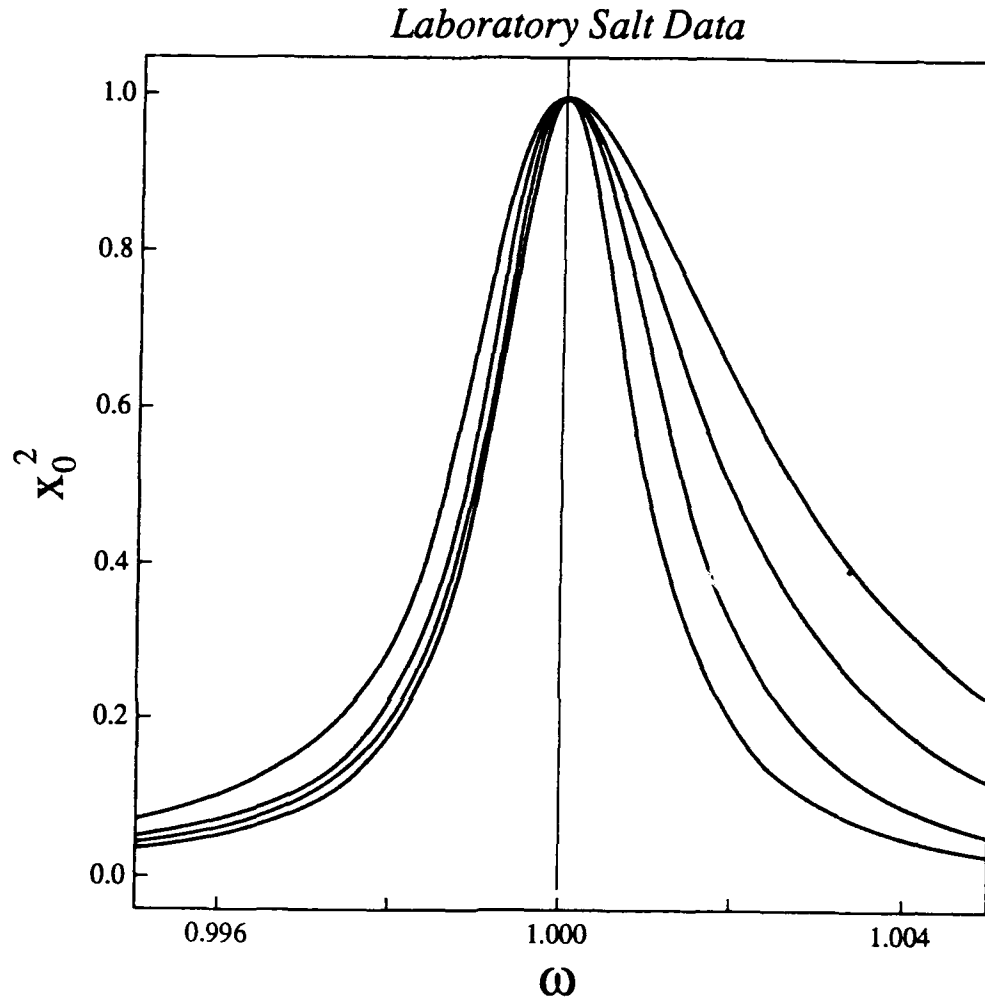


Fig. 2. Distorted Lorentz peaks obtained from flexure experiments in dome salt. Data generated by *Bulau and Tittman* [1983, personal communication]. Samples were flexed at 480 Hz under 1.36×10^7 Pa effective pressure. Each resonance curve has been rescaled and aligned to a common peak for this plot, in order to illustrate the distortion at large strain amplitude. In order of increasing strain amplitude, the four curves correspond to a) $\epsilon = 1.3 \cdot 10^{-7}$, $Q = 495$, b) $\epsilon = 6.5 \cdot 10^{-7}$, $Q = 403$, c) $\epsilon = 2.6 \cdot 10^{-6}$, $Q = 319$, d) $\epsilon = 6.3 \cdot 10^{-6}$, $Q = 242$, where Q is estimated from the peak width at half-power.

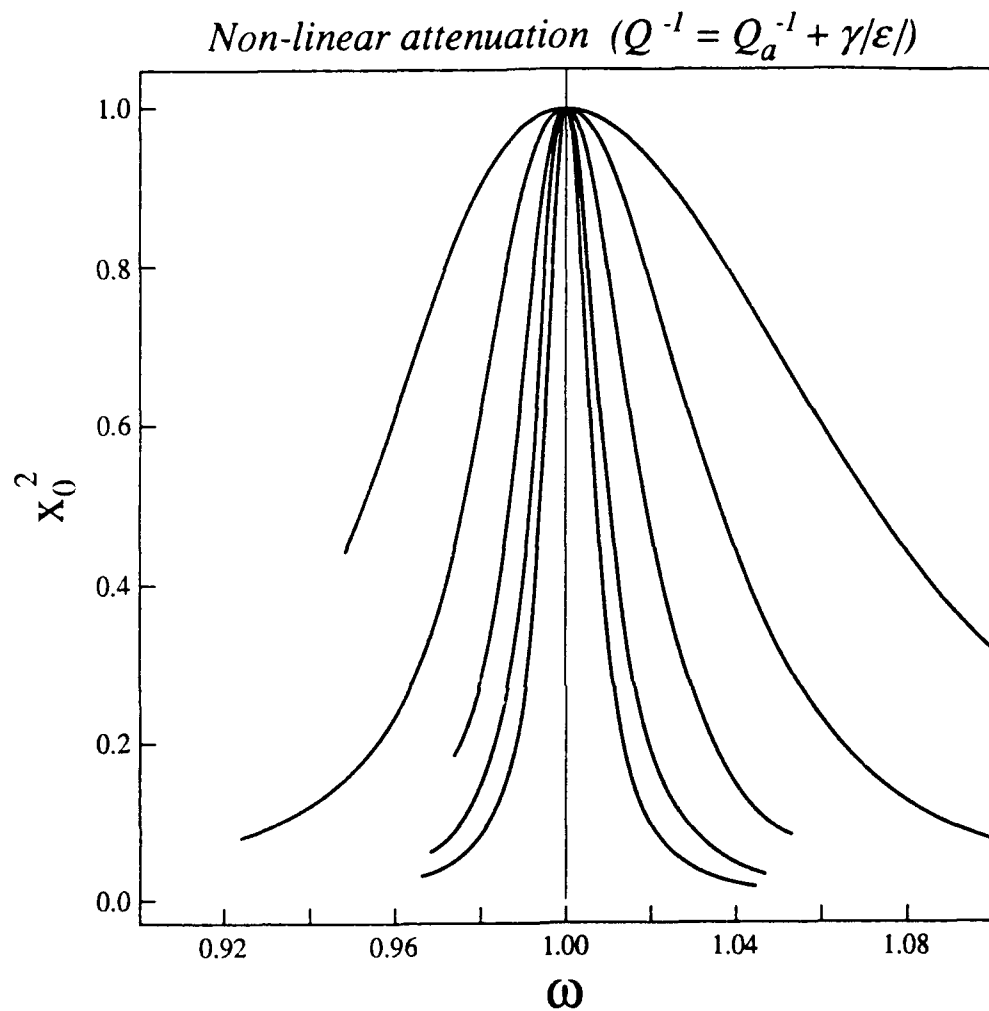


Fig. 3. Synthetic Lorentz peaks obtained from a numerical simulation of a simple harmonic oscillator with attenuation varying as $Q^{-1} = 0.01 + 140 \epsilon$, where ϵ is the strain amplitude.

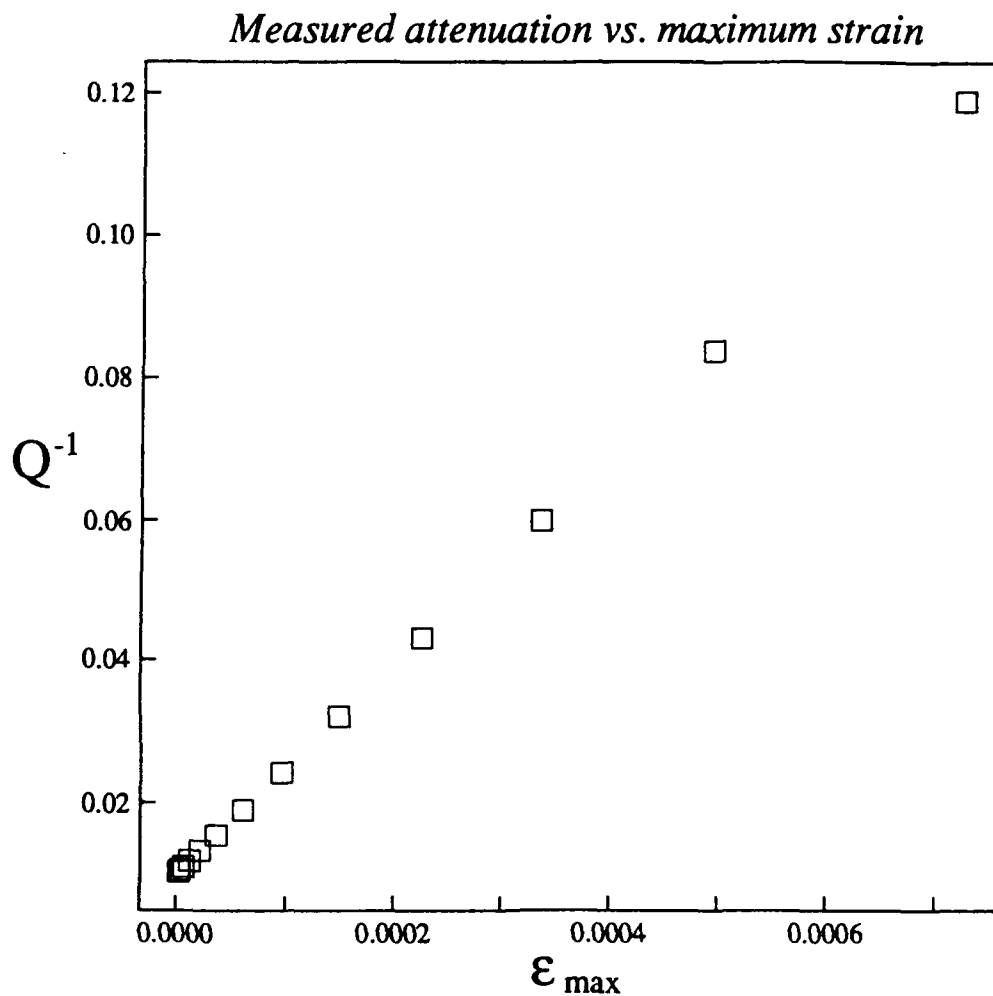


Fig. 4. Attenuation as measured from the curves shown in Fig. 3 using the relation $Q^{-1} = (\omega_2 - \omega_1)/\omega_r$ at the half-power level, plotted against maximum strain amplitude. Apparent Q^{-1} varies linearly with ϵ_{\max} . The slope of this line implies a γ value of about 150, very close to the actual value of 140 used to generate the curves shown in Fig. 3.

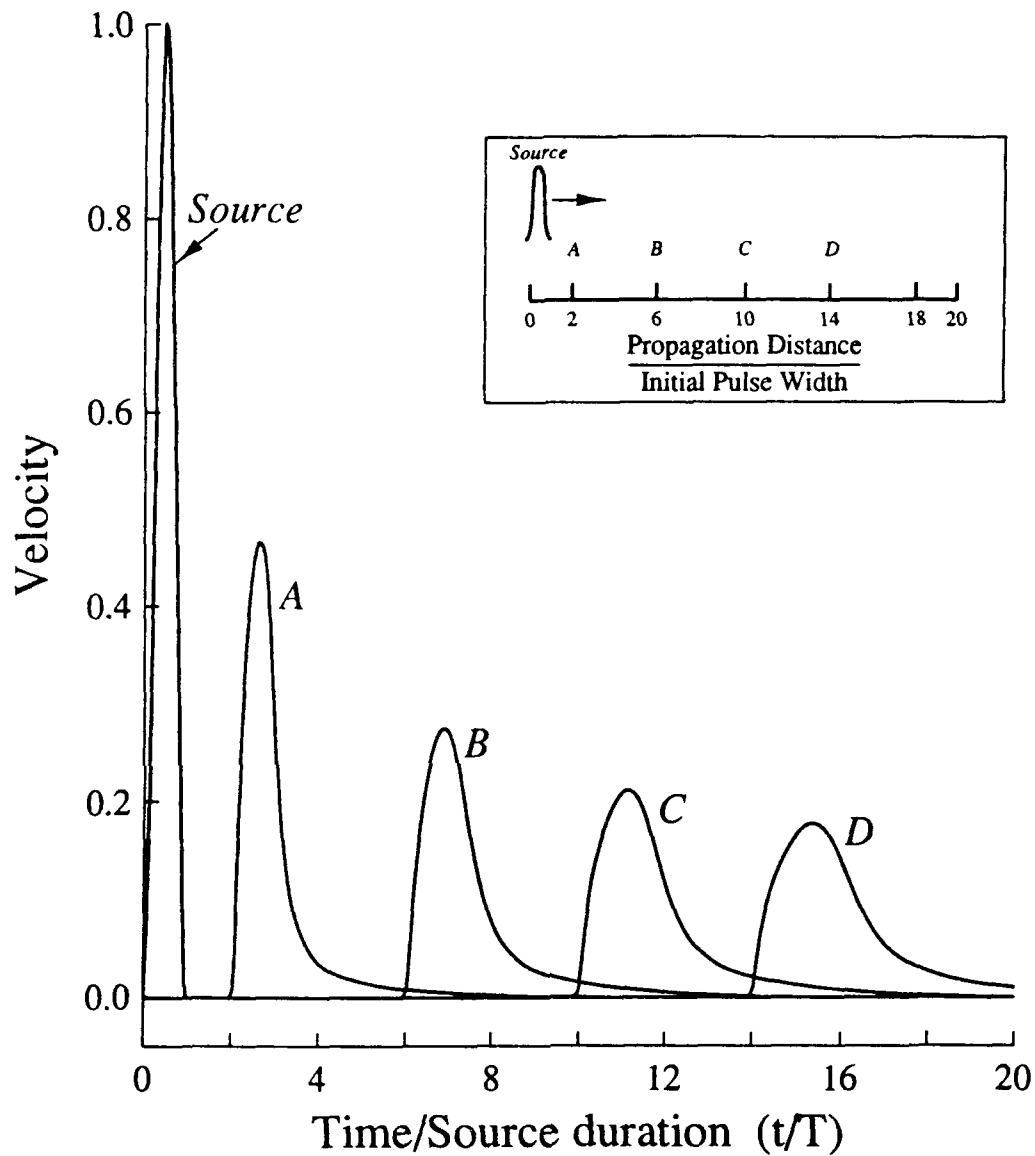


Fig. 5. Velocity time histories at four propagation distances, for a nonlinear simulation with Q_a equal to 1000 and $\gamma \times \epsilon_{max}$ equal to 0.3. A plane wave is incident from one direction, as shown. The prescribed time history at distance 0 is shown at the far left; all times are scaled to the source duration, T , and all distances are scaled to the product of wavespeed and source duration, cT .

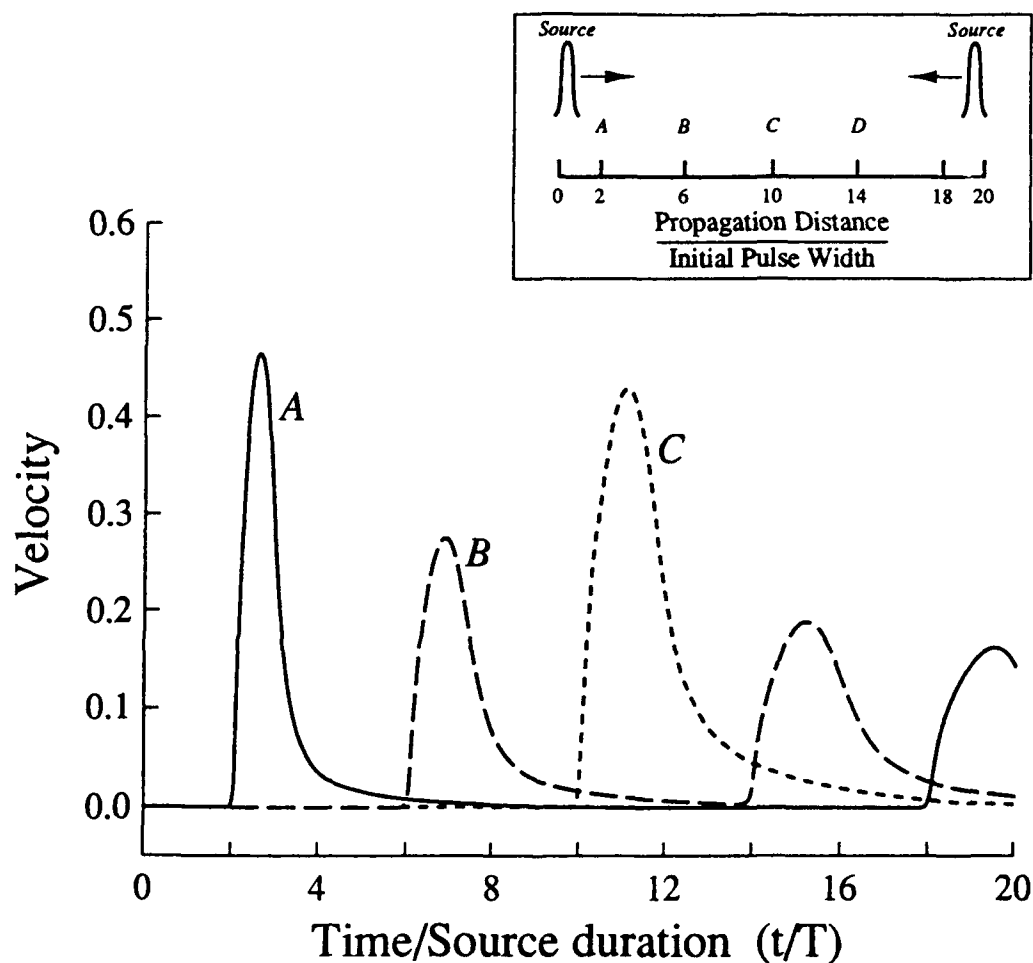


Fig. 6. Velocity time histories at three propagation distances, for a nonlinear simulation with Q_a equal to 1000 and $\gamma \times \epsilon_{max}$ equal to 0.3, as in the previous figure. In this case, however, plane waves are incident from both directions. Location C is the midpoint between the source points. Times and distances are scaled as in the previous figure.

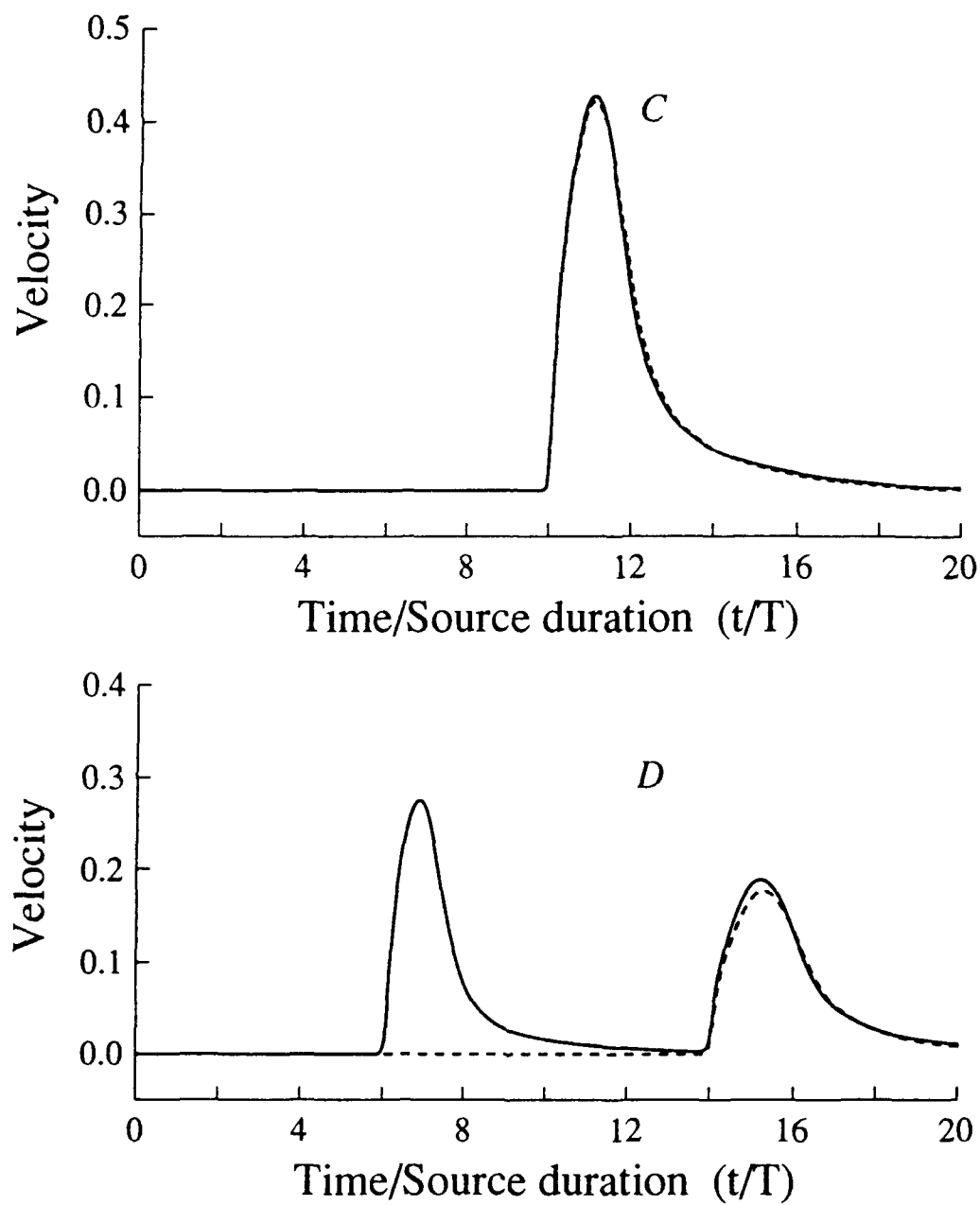


Fig. 7. (a) The velocity time histories at location C (midpoint). Results are compared for the single source simulation, multiplied by 2 (dashed curve), and the interfering sources simulation (solid curve). (b) Same as (a), but for location B.

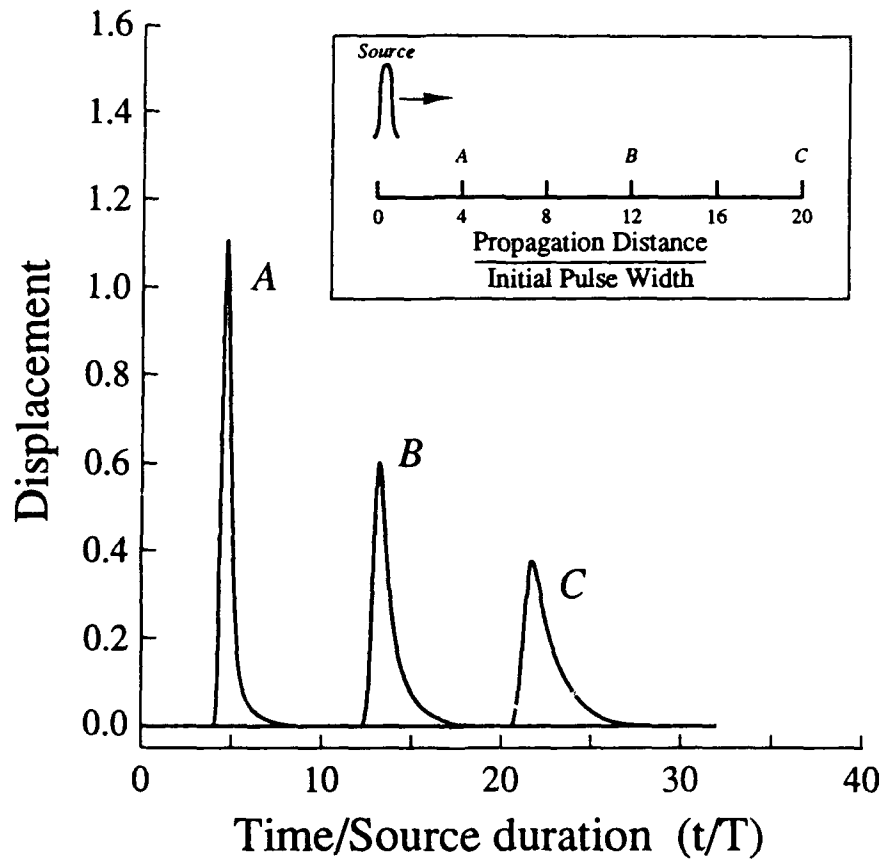


Fig. 8. Displacement time histories for a linear (amplitude-independent Q) simulation, with Q equal to 20. The source time history is the derivative of that shown in Figure 5 (i.e., the source *displacement* has the same form as the source *velocity* shown in Figure 5).

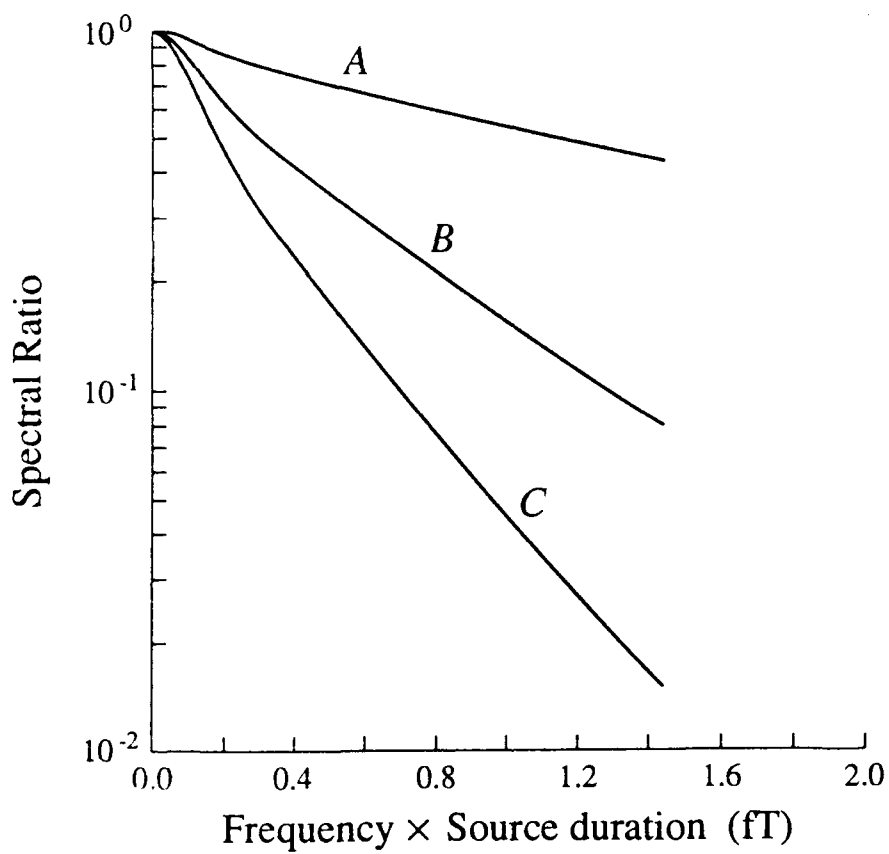


Fig. 9. Spectral ratios for the amplitude-independent Q simulation shown in Figure 8. Each curve is the spectral amplitude of the corresponding displacement time history from Figure 8, divided by the spectral amplitude of the source displacement.

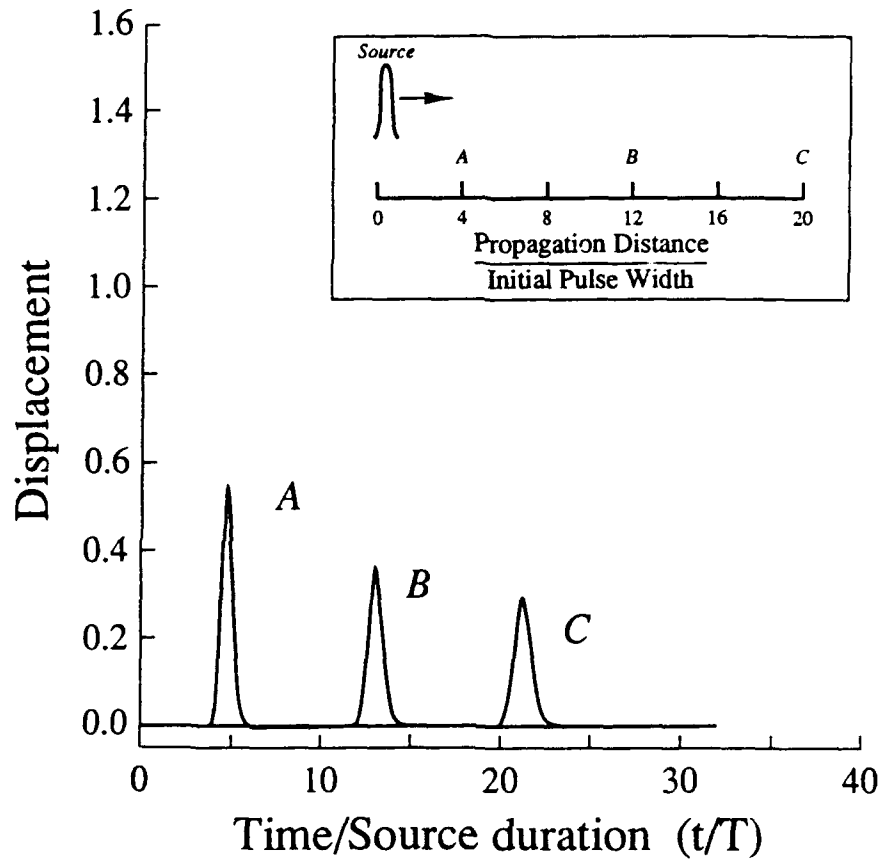


Fig. 10. Displacement time histories for an amplitude-dependent Q simulation, with Q_a equal to 1000 and the product $[\gamma \times \epsilon_{max}]$ equal to 0.3. The source prescription is the same as for the linear simulation depicted in Figure 8.

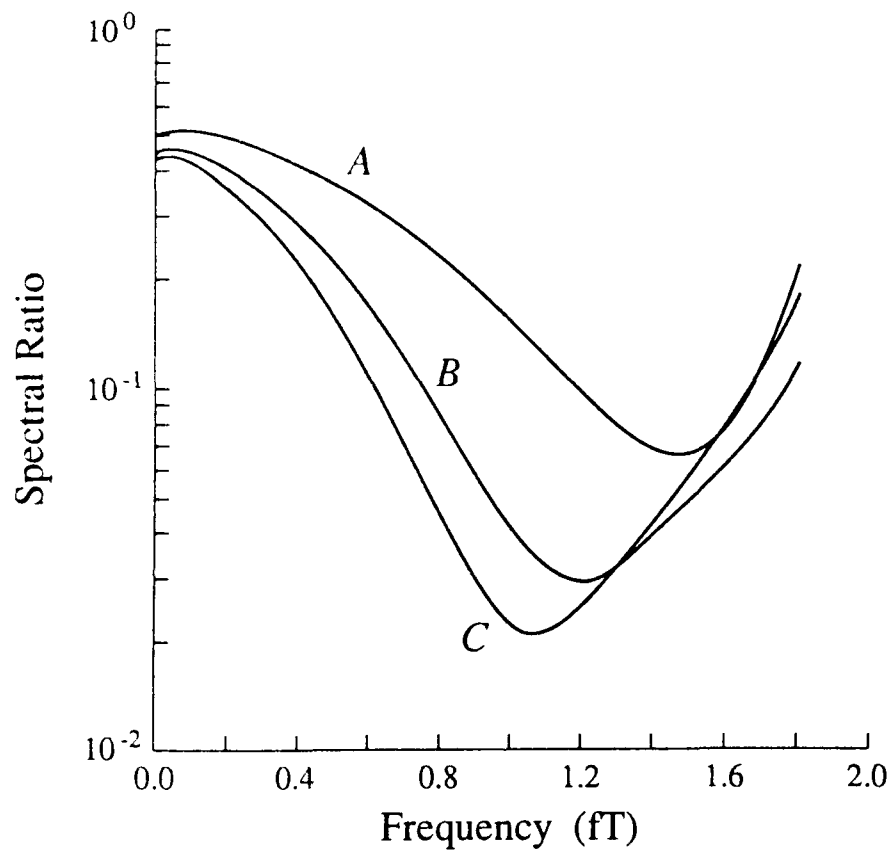


Fig. 11. Spectral ratios for the amplitude-dependent Q simulations shown in Figure 10. Each curve is the spectral amplitude of the corresponding displacement time history from Figure 10, divided by the spectral amplitude of the source displacement.

Prof. Thomas Ahrens
Seismological Lab, 252-21
Division of Geological & Planetary Sciences
California Institute of Technology
Pasadena, CA 91125

Prof. Charles B. Archambeau
CIRES
University of Colorado
Boulder, CO 80309

Dr. Thomas C. Bache, Jr.
Science Applications Int'l Corp.
10260 Campus Point Drive
San Diego, CA 92121 (2 copies)

Prof. Muawia Barazangi
Institute for the Study of the Continent
Cornell University
Ithaca, NY 14853

Dr. Douglas R. Baumgardt
ENSCO, Inc
5400 Port Royal Road
Springfield, VA 22151-2388

Prof. Jonathan Berger
IGPP, A-025
Scripps Institution of Oceanography
University of California, San Diego
La Jolla, CA 92093

Dr. Lawrence J. Burdick
Woodward-Clyde Consultants
566 El Dorado Street
Pasadena, CA 91109-3245

Dr. Jerry Carter
Center for Seismic Studies
1300 North 17th St., Suite 1450
Arlington, VA 22209-2308

Dr. Karl Coyner
New England Research, Inc.
76 Olcott Drive
White River Junction, VT 05001

Prof. Vernon F. Cormier
Department of Geology & Geophysics
U-45, Room 207
The University of Connecticut
Storrs, CT 06268

Professor Anton W. Dainty
Earth Resources Laboratory
Massachusetts Institute of Technology
42 Carleton Street
Cambridge, MA 02142

Prof. Steven Day
Department of Geological Sciences
San Diego State University
San Diego, CA 92182

Dr. Zoltan A. Der
ENSCO, Inc.
5400 Port Royal Road
Springfield, VA 22151-2388

Prof. John Ferguson
Center for Lithospheric Studies
The University of Texas at Dallas
P.O. Box 830688
Richardson, TX 75083-0688

Dr. Mark D. Fisk
Mission Research Corporation
735 State Street
P. O. Drawer 719
Santa Barbara, CA 93102

Prof. Stanley Flatte
Applied Sciences Building
University of California
Santa Cruz, CA 95064

Dr. Alexander Florence
SRI International
333 Ravenswood Avenue
Menlo Park, CA 94025-3493

Prof. Henry L. Gray
Vice Provost and Dean
Department of Statistical Sciences
Southern Methodist University
Dallas, TX 75275

Dr. Indra Gupta
Teledyne Geotech
314 Montgomery Street
Alexandria, VA 22314

Prof. David G. Harkrider
Seismological Laboratory
Division of Geological & Planetary Sciences
California Institute of Technology
Pasadena, CA 91125

Prof. Donald V. Helmberger
Seismological Laboratory
Division of Geological & Planetary Sciences
California Institute of Technology
Pasadena, CA 91125

Prof. Eugene Herrin
Institute for the Study of Earth and Man
Geophysical Laboratory
Southern Methodist University
Dallas, TX 75275

Prof. Bryan Isacks
Cornell University
Department of Geological Sciences
SNEE Hall
Ithaca, NY 14850

Dr. Rong-Song Jih
Teledyne Geotech
314 Montgomery Street
Alexandria, VA 22314

Prof. Lane R. Johnson
Seismographic Station
University of California
Berkeley, CA 94720

Dr. Richard LaCoss
MIT-Lincoln Laboratory
M-200B
P. O. Box 73
Lexington, MA 02173-0073 (3 copies)

Prof Fred K. Lamb
University of Illinois at Urbana-Champaign
Department of Physics
1110 West Green Street
Urbana, IL 61801

Prof. Charles A. Langston
Geosciences Department
403 Deike Building
The Pennsylvania State University
University Park, PA 16802

Prof. Thorne Lay
Institute of Tectonics
Earth Science Board
University of California, Santa Cruz
Santa Cruz, CA 95064

Prof. Arthur Lerner-Lam
Lamont-Doherty Geological Observatory
of Columbia University
Palisades, NY 10964

Dr. Christopher Lynnes
Teledyne Geotech
314 Montgomery Street
Alexandria, VA 22314

Professor Peter E. Malin
Department of Geology
Old Chemistry Building
Duke University
Durham, NC 27706

Dr. Randolph Martin, III
New England Research, Inc.
76 Olcott Drive
White River Junction, VT 05001

Prof. Thomas V. McEvilly
Seismographic Station
University of California
Berkeley, CA 94720

Dr. Keith L. McLaughlin
S-CUBED
A Division of Maxwell Laboratory
P.O. Box 1620
La Jolla, CA 92038-1620

Prof. William Menke
Lamont-Doherty Geological Observatory
of Columbia University
Palisades, NY 10964

Stephen Miller
SRI International
333 Ravenswood Avenue
Box AF 116
Menlo Park, CA 94025-3493

Prof. Bernard Minster
IGPP, A-025
Scripps Institute of Oceanography
University of California, San Diego
La Jolla, CA 92093

Prof. Brian J. Mitchell
Department of Earth & Atmospheric Sciences
St. Louis University
St. Louis, MO 63156

Mr. Jack Murphy
S-CUBED, A Division of Maxwell Laboratory
11800 Sunrise Valley Drive
Suite 1212
Reston, VA 22091 (2 copies)

Prof. John A. Orcutt
IGPP, A-025
Scripps Institute of Oceanography
University of California, San Diego
La Jolla, CA 92093

Prof. Keith Priestley
University of Cambridge
Bullard Labs, Dept. of Earth Sciences
Madingley Rise, Madingley Rd.
Cambridge CB3 0EZ, ENGLAND

Dr. Jay J. Pulli
Radix Systems, Inc.
2 Taft Court, Suite 203
Rockville, MD 20850

Prof. Paul G. Richards
Lamont-Doherty Geological Observatory
of Columbia University
Palisades, NY 10964

Dr. Wilmer Rivers
Teledyne Geotech
314 Montgomery Street
Alexandria, VA 22314

Prof. Charles G. Sammis
Center for Earth Sciences
University of Southern California
University Park
Los Angeles, CA 90089-0741

Prof. Christopher H. Scholz
Lamont-Doherty Geological Observatory
of Columbia University
Palisades, NY 10964

Thomas J. Sereno, Jr.
Science Application Int'l Corp.
10260 Campus Point Drive
San Diego, CA 92121

Prof. David G. Simpson
Lamont-Doherty Geological Observatory
of Columbia University
Palisades, NY 10964

Dr. Jeffrey Stevens
S-CUBED
A Division of Maxwell Laboratory
P.O. Box 1620
La Jolla, CA 92038-1620

Prof. Brian Stump
Institute for the Study of Earth & Man
Geophysical Laboratory
Southern Methodist University
Dallas, TX 75275

Prof. Jeremiah Sullivan
University of Illinois at Urbana-Champaign
Department of Physics
1110 West Green Street
Urbana, IL 61801

Prof. Clifford Thurber
University of Wisconsin-Madison
Department of Geology & Geophysics
1215 West Dayton Street
Madison, WI 53706

Prof. M. Nafi Toksoz
Earth Resources Lab
Massachusetts Institute of Technology
42 Carleton Street
Cambridge, MA 02142

Prof. John E. Vidale
University of California at Santa Cruz
Seismological Laboratory
Santa Cruz, CA 95064

Prof. Terry C. Wallace
Department of Geosciences
Building #77
University of Arizona
Tucson, AZ 85721

Dr. William Wortman
Mission Research Corporation
735 State Street
P. O. Drawer 719
Santa Barbara, CA 93102

OTHERS (UNITED STATES)

Dr. Monem Abdel-Gawad
Rockwell International Science Center
1049 Camino Dos Rios
Thousand Oaks, CA 91360

Prof. Keiiti Aki
Center for Earth Sciences
University of Southern California
University Park
Los Angeles, CA 90089-0741

Prof. Shelton S. Alexander
Geosciences Department
403 Deike Building
The Pennsylvania State University
University Park, PA 16802

Dr. Kenneth Anderson
BBNSTC
Mail Stop 14/1B
Cambridge, MA 02238

Dr. Ralph Archuleta
Department of Geological Sciences
University of California at Santa Barbara
Santa Barbara, CA 93102

Dr. Jeff Barker
Department of Geological Sciences
State University of New York
at Binghamton
Vestal, NY 13901

Dr. Susan Beck
Department of Geosciences
Bldg. # 77
University of Arizona
Tucson, AZ 85721

Dr. T.J. Bennett
S-CUBED
A Division of Maxwell Laboratory
11800 Sunrise Valley Drive, Suite 1212
Reston, VA 22091

Mr. William J. Best
907 Westwood Drive
Vienna, VA 22180

Dr. N. Biswas
Geophysical Institute
University of Alaska
Fairbanks, AK 99701

Dr. G.A. Bollinger
Department of Geological Sciences
Virginia Polytechnical Institute
21044 Derring Hall
Blacksburg, VA 24061

Dr. Stephen Bratt
Center for Seismic Studies
1300 North 17th Street
Suite 1450
Arlington, VA 22209

Michael Browne
Teledyne Geotech
3401 Shiloh Road
Garland, TX 75041

Mr. Roy Burger
1221 Serry Road
Schenectady, NY 12309

Dr. Robert Burrige
Schlumberger-Doll Research Center
Old Quarry Road
Ridgefield, CT 06877

Dr. W. Winston Chan
Teledyne Geotech
314 Montgomery Street
Alexandria, VA 22314-1581

Dr. Theodore Cherry
Science Horizons, Inc.
710 Encinitas Blvd., Suite 200
Encinitas, CA 92024 (2 copies)

Prof. Jon F. Claerbout
Department of Geophysics
Stanford University
Stanford, CA 94305

Prof. Robert W. Clayton
Seismological Laboratory
Division of Geological & Planetary Sciences
California Institute of Technology
Pasadena, CA 91125

Prof. F. A. Dahlen
Geological and Geophysical Sciences
Princeton University
Princeton, NJ 08544-0636

Mr. Charles Doll
Earth Resources Laboratory
Massachusetts Institute of Technology
42 Carleton St.
Cambridge, MA 02142

Prof. Adam Dziewonski
Hoffman Laboratory
Harvard University
20 Oxford St
Cambridge, MA 02138

Prof. John Ebel
Department of Geology & Geophysics
Boston College
Chestnut Hill, MA 02167

Eric Fielding
SNEE Hall
INSTOC
Cornell University
Ithaca, NY 14853

Dr. John Foley
GL/LWH
Hanscom AFB, MA 01731-5000

Prof. Donald Forsyth
Department of Geological Sciences
Brown University
Providence, RI 02912

Dr. Cliff Frolich
Institute of Geophysics
8701 North Mopac
Austin, TX 78759

Dr. Anthony Gangi
Texas A&M University
Department of Geophysics
College Station, TX 77843

Dr. Freeman Gilbert
IGPP, A-025
Scripps Institute of Oceanography
University of California
La Jolla, CA 92093

Mr. Edward Giller
Pacific Sierra Research Corp.
1401 Wilson Boulevard
Arlington, VA 22209

Dr. Jeffrey W. Given
SAIC
10260 Campus Point Drive
San Diego, CA 92121

Prof. Stephen Grand
University of Texas at Austin
Department of Geological Sciences
Austin, TX 78713-7909

Prof. Roy Greenfield
Geosciences Department
403 Deike Building
The Pennsylvania State University
University Park, PA 16802

Dan N. Hagedorn
Battelle
Pacific Northwest Laboratories
Battelle Boulevard
Richland, WA 99352

Dr. James Hannon
Lawrence Livermore National Laboratory
P. O. Box 808
Livermore, CA 94550

Prof. Robert B. Herrmann
Dept. of Earth & Atmospheric Sciences
St. Louis University
St. Louis, MO 63156

Ms. Heidi Houston
Seismological Laboratory
University of California
Santa Cruz, CA 95064

Kevin Hutchenson
Department of Earth Sciences
St. Louis University
3507 Laclede
St. Louis, MO 63103

Dr. Hans Israelsson
Center for Seismic Studies
1300 N. 17th Street, Suite 1450
Arlington, VA 22209-2308

Prof. Thomas H. Jordan
Department of Earth, Atmospheric
and Planetary Sciences
Massachusetts Institute of Technology
Cambridge, MA 02139

Prof. Alan Kafka
Department of Geology & Geophysics
Boston College
Chestnut Hill, MA 02167

Robert C. Kemerait
ENSCO, Inc.
445 Pineda Court
Melbourne, FL 32940

William Kikendall
Teledyne Geotech
3401 Shiloh Road
Garland, TX 75041

Prof. Leon Knopoff
University of California
Institute of Geophysics & Planetary Physics
Los Angeles, CA 90024

Prof. L. Timothy Long
School of Geophysical Sciences
Georgia Institute of Technology
Atlanta, GA 30332

Dr. Gary McCartor
Department of Physics
Southern Methodist University
Dallas, TX 75275

Prof. Art McGarr
Mail Stop 977
Geological Survey
345 Middlefield Rd.
Menlo Park, CA 94025

Dr. George Mellman
Sierra Geophysics
11255 Kirkland Way
Kirkland, WA 98033

Prof. John Nabelek
College of Oceanography
Oregon State University
Corvallis, OR 97331

Prof. Geza Nagy
University of California, San Diego
Department of Ames, M.S. B-010
La Jolla, CA 92093

Dr. Keith K. Nakanishi
Lawrence Livermore National Laboratory
L-205
P. O. Box 808
Livermore, CA 94550

Dr. Bao Nguyen
GL/LWH
Hanscom AFB, MA 01731-5000

Prof. Amos Nur
Department of Geophysics
Stanford University
Stanford, CA 94305

Prof. Jack Oliver
Department of Geology
Cornell University
Ithaca, NY 14850

Dr. Kenneth Olsen
P. O. Box 1273
Linwood, WA 98046-1273

Howard J. Patton
Lawrence Livermore National Laboratory
L-205
P. O. Box 808
Livermore, CA 94550

Prof. Robert Phinney
Geological & Geophysical Sciences
Princeton University
Princeton, NJ 08544-0636

Dr. Paul Pomeroy
Rondout Associates
P.O. Box 224
Stone Ridge, NY 12484

Dr. Jay Pulli
RADIX System, Inc.
2 Taft Court, Suite 203
Rockville, MD 20850

Dr. Norton Rimer
S-CUBED
A Division of Maxwell Laboratory
P.O. Box 1620
La Jolla, CA 92038-1620

Prof. Larry J. Ruff
Department of Geological Sciences
1006 C.C. Little Building
University of Michigan
Ann Arbor, MI 48109-1063

Dr. Richard Sailor
TASC Inc.
55 Walkers Brook Drive
Reading, MA 01867

Dr. Susan Schwartz
Institute of Tectonics
1156 High St.
Santa Cruz, CA 95064

John Sherwin
Teledyne Geotech
3401 Shiloh Road
Garland, TX 75041

Dr. Matthew Sibol
Virginia Tech
Seismological Observatory
4044 Derring Hall
Blacksburg, VA 24061-0420

Dr. Albert Smith
Lawrence Livermore National Laboratory
L-205
P. O. Box 808
Livermore, CA 94550

Prof. Robert Smith
Department of Geophysics
University of Utah
1400 East 2nd South
Salt Lake City, UT 84112

Dr. Stewart W. Smith
Geophysics AK-50
University of Washington
Seattle, WA 98195

Donald L. Springer
Lawrence Livermore National Laboratory
L-205
P. O. Box 808
Livermore, CA 94550

Dr. George Sutton
Rondout Associates
P.O. Box 224
Stone Ridge, NY 12484

Prof. L. Sykes
Lamont-Doherty Geological Observatory
of Columbia University
Palisades, NY 10964

Prof. Pradeep Talwani
Department of Geological Sciences
University of South Carolina
Columbia, SC 29208

Dr. David Taylor
ENSCO, Inc.
445 Pineda Court
Melbourne, FL 32940

Dr. Steven R. Taylor
Lawrence Livermore National Laboratory
L-205
P. O. Box 808
Livermore, CA 94550

Professor Ta-Liang Teng
Center for Earth Sciences
University of Southern California
University Park
Los Angeles, CA 90089-0741

Dr. R.B. Tittmann
Rockwell International Science Center
1049 Camino Dos Rios
P.O. Box 1085
Thousand Oaks, CA 91360

Dr. Gregory van der Vink
IRIS, Inc.
1616 North Fort Myer Drive
Suite 1440
Arlington, VA 22209

Professor Daniel Walker
University of Hawaii
Institute of Geophysics
Honolulu, HI 96822

William R. Walter
Seismological Laboratory
University of Nevada
Reno, NV 89557

Dr. Raymond Willeman
GL/LWH
Hanscom AFB, MA 01731-5000

Dr. Gregory Wojcik
Weidlinger Associates
4410 El Camino Real
Suite 110
Los Altos, CA 94022

Dr. Lorraine Wolf
GL/LWH
Hanscom AFB, MA 01731-5000

Prof. Francis T. Wu
Department of Geological Sciences
State University of New York
at Binghamton
Vestal, NY 13901

Dr. Gregory B. Young
ENSCO, Inc.
5400 Port Royal Road
Springfield, VA 22151-2388

Dr. Eileen Vergino
Lawrence Livermore National Laboratory
L-205
P. O. Box 808
Livermore, CA 94550

J. J. Zucca
Lawrence Livermore National Laboratory
P. O. Box 808
Livermore, CA 94550

GOVERNMENT

Dr. Ralph Alewine III
DARPA/NMRO
1400 Wilson Boulevard
Arlington, VA 22209-2308

Mr. James C. Battis
GL/LWH
Hanscom AFB, MA 01731-5000

Dr. Robert Blandford
AFTAC/IT
Center for Seismic Studies
1300 North 17th St., Suite 1450
Arlington, VA 22209-2308

Eric Chael
Division 9241
Sandia Laboratory
Albuquerque, NM 87185

Dr. John J. Cipar
GL/LWH
Hanscom AFB, MA 01731-5000

Cecil Davis
Group P-15, Mail Stop D406
P.O. Box 1663
Los Alamos National Laboratory
Los Alamos, NM 87544

Mr. Jeff Duncan
Office of Congressman Markey
2133 Rayburn House Bldg.
Washington, DC 20515

Dr. Jack Evernden
USGS - Earthquake Studies
345 Middlefield Road
Menlo Park, CA 94025

Art Frankel
USGS
922 National Center
Reston, VA 22092

Dr. Dale Glover
DIA/DT-1B
Washington, DC 20301

Dr. T. Hanks
USGS
Nat'l Earthquake Research Center
345 Middlefield Road
Menlo Park, CA 94025

Paul Johnson
ESS-4, Mail Stop J979
Los Alamos National Laboratory
Los Alamos, NM 87545

Janet Johnston
GL/LWH
Hanscom AFB, MA 01731-5000

Dr. Katharine Kadinsky-Cade
GL/LWH
Hanscom AFB, MA 01731-5000

Ms. Ann Kerr
IGPP, A-025
Scripps Institute of Oceanography
University of California, San Diego
La Jolla, CA 92093

Dr. Max Koontz
US Dept of Energy/DP 5
Forrestal Building
1000 Independence Avenue
Washington, DC 20585

Dr. W.H.K. Lee
Office of Earthquakes, Volcanoes,
& Engineering
345 Middlefield Road
Menlo Park, CA 94025

Dr. William Leith
U.S. Geological Survey
Mail Stop 928
Reston, VA 22092

Dr. Richard Lewis
Director, Earthquake Engineering & Geophysics
U.S. Army Corps of Engineers
Box 631
Vicksburg, MS 39180

James F. Lewkowicz
GL/LWH
Hanscom AFB, MA 01731-5000

Mr. Alfred Lieberman
ACDA/VI-OA'State Department Bldg
Room 5726
320 - 21st Street, NW
Washington, DC 20451

Stephen Mangino
GL/LWH
Hanscom AFB, MA 01731-5000

Dr. Robert Masse
Box 25046, Mail Stop 967
Denver Federal Center
Denver, CO 80225

Art McGarr
U.S. Geological Survey, MS-977
345 Middlefield Road
Menlo Park, CA 94025

Richard Morrow
ACDA/VI, Room 5741
320 21st Street N.W
Washington, DC 20451

Dr. Carl Newton
Los Alamos National Laboratory
P.O. Box 1663
Mail Stop C335, Group ESS-3
Los Alamos, NM 87545

Dr. Kenneth H. Olsen
Los Alamos Scientific Laboratory
P. O. Box 1663
Mail Stop D-406
Los Alamos, NM 87545

Mr. Chris Paine
Office of Senator Kennedy
SR 315
United States Senate
Washington, DC 20510

Colonel Jerry J. Perrizo
AFOSR/NP, Building 410
Bolling AFB
Washington, DC 20332-6448

Dr. Frank F. Pilotte
HQ AFTAC/TT
Patrick AFB, FL 32925-6001

Katie Poley
CIA-ACIS/TMC
Room 4X16NHB
Washington, DC 20505

Mr. Jack Rachlin
U.S. Geological Survey
Geology, Rm 3 C136
Mail Stop 928 National Center
Reston, VA 22092

Dr. Robert Reinke
WL/NTESG
Kirtland AFB, NM 87117-6008

Dr. Byron Ristvet
HQ DNA, Nevada Operations Office
Attn: NVCG
P.O. Box 98539
Las Vegas, NV 89193

Dr. George Rothe
HQ AFTAC/TTR
Patrick AFB, FL 32925-6001

Dr. Alan S. Ryall, Jr.
DARPA/NMRO
1400 Wilson Boulevard
Arlington, VA 22209-2308

Dr. Michael Shore
Defense Nuclear Agency/SPSS
6801 Telegraph Road
Alexandria, VA 22310

Mr. Charles L. Taylor
GL/LWG
Hanscom AFB, MA 01731-5000

Dr. Larry Turnbull
CIA-OSWR/NED
Washington, DC 20505

Dr. Thomas Weaver
Los Alamos National Laboratory
P.O. Box 1663, Mail Stop C335
Los Alamos, NM 87545

GI/SULL
Research Library
Hanscom AFB , MA 01731-5000 (2 copies)

Defense Intelligence Agency
Directorate for Scientific & Technical Intelligence
Attn: DT1B
Washington, DC 20340-6158

Secretary of the Air Force
(SAFRD)
Washington, DC 20330

AFTAC/CA
(STINFO)
Patrick AFB, FL 32925-6001

Office of the Secretary Defense
DDR & E
Washington, DC 20330

TACTEC
Battelle Memorial Institute
505 King Avenue
Columbus, OH 43201 (Final Report Only)

HQ DNA
Attn: Technical Library
Washington, DC 20305

DARPA/RMO/RETRIEVAL
1400 Wilson Boulevard
Arlington, VA 22209

DARPA/RMO/Security Office
1400 Wilson Boulevard
Arlington, VA 22209

Geophysics Laboratory
Attn: XO
Hanscom AFB, MA 01731-5000

Geophysics Laboratory
Attn: LW
Hanscom AFB, MA 01731-5000

DARPA/PM
1400 Wilson Boulevard
Arlington, VA 22209

Defense Technical Information Center
Cameron Station
Alexandria, VA 22314 (5 copies)

CONTRACTORS (FOREIGN)

Dr. Ramon Cabre, S.J.
Observatorio San Calixto
Casilla 5939
La Paz, Bolivia

Prof. Hans-Peter Harjes
Institute for Geophysik
Ruhr University/Bochum
P.O. Box 102148
4630 Bochum 1, FRG

Prof. Eystein Husebye
NTNF/NORSAR
P.O. Box 51
N-2007 Kjeller, NORWAY

Prof. Brian L.N. Kennett
Research School of Earth Sciences
Institute of Advanced Studies
G.P.O. Box 4
Canberra 2601, AUSTRALIA

Dr. Bernard Massinon
Societe Radiomana
27 rue Claude Bernard
75005 Paris, FRANCE (2 Copies)

Dr. Pierre Mecheler
Societe Radiomana
27 rue Claude Bernard
75005 Paris, FRANCE

Dr. Svein Mykkeltveit
NTNF/NORSAR
P.O. Box 51
N-2007 Kjeller, NORWAY (3 copies)

FOREIGN (OTHERS)

Dr. Peter Basham
Earth Physics Branch
Geological Survey of Canada
1 Observatory Crescent
Ottawa, Ontario, CANADA K1A 0Y3

Dr. Eduard Berg
Institute of Geophysics
University of Hawaii
Honolulu, HI 96822

Dr. Michel Bouchon
I.R.I.G.M.-B.P. 68
38402 St. Martin D'Herès
Cedex, FRANCE

Dr. Helmar Bungum
NTNF/NORSAR
P.O. Box 51
N-2007 Kjeller, NORWAY

Dr. Michel Campillo
Observatoire de Grenoble
I.R.I.G.M.-B.P. 53
38041 Grenoble, FRANCE

Dr. Kin Yip Chun
Geophysics Division
Physics Department
University of Toronto
Ontario, CANADA M5S 1A7

Dr. Alan Douglas
Ministry of Defense
Blacknest, Brimpton
Reading RG7-4RS, UNITED KINGDOM

Dr. Roger Hansen
NTNF/NORSAR
P.O. Box 51
N-2007 Kjeller, NORWAY

Dr. Manfred Henger
Federal Institute for Geosciences & Nat'l Res.
Postfach 510153
D-3000 Hanover 51, FRG

Ms. Eva Johannisson
Senior Research Officer
National Defense Research Inst.
P.O. Box 27322
S-102 54 Stockholm, SWEDEN

Dr. Fekadu Kebede
Geophysical Observatory, Science Faculty
Addis Ababa University
P. O. Box 1176
Addis Ababa, ETHIOPIA

Dr. Tormod Kvaerna
NTNF/NORSAR
P.O. Box 51
N-2007 Kjeller, NORWAY

Dr. Peter Marshall
Procurement Executive
Ministry of Defense
Blacknest, Brimpton
Reading FG7-4RS, UNITED KINGDOM

Prof. Ari Ben-Menahem
Department of Applied Mathematics
Weizman Institute of Science
Rehovot, ISRAEL 951729

Dr. Robert North
Geophysics Division
Geological Survey of Canada
1 Observatory Crescent
Ottawa, Ontario, CANADA K1A 0Y3

Dr. Frode Ringdal
NTNF/NORSAR
P.O. Box 51
N-2007 Kjeller, NORWAY

Dr. Jorg Schlittenhardt
Federal Institute for Geosciences & Nat'l Res.
Postfach 510153
D-3000 Hannover 51, FEDERAL REPUBLIC OF GERMANY

Universita Degli Studi Di Trieste
Facolta Di Ingegneria
Istituto Di Miniere E. Geofisica Applicata, Trieste, ITALY